UNIVERSITY OF CALIFORNIA
RIVERSIDE

Evaluating Behavioral Phenotypes and FMRP Expression in a Developmental Astrocyte-Specific Mouse Model of Fragile X Syndrome

A Thesis submitted in partial satisfaction
of the requirements for the degree of

Master of Science

in

Biomedical Sciences

by

Alexandra Varallo

June 2024

Thesis Committee:
Dr. Iryna Ethell, Committee Chairperson
Dr. Khaleel Razak
Dr. Djurdjica Coss

The Thesis of Alexandra Varallo is approved:

Committee Chairperson

University of California, Riverside

ACKNOWLEDGEMENTS

I would like to warmly thank my thesis advisor and committee chairperson, Dr. Iryna Ethell, for her guidance and support on this project. I would also like to thank Victoria Wagner, Dr. Anna Kulinich, and Dr. Samantha Sutley-Koury for their guidance, mentorship, and informative discussions. I am also very thankful for the support of my family, friends, and colleagues from the Biomedical Sciences and Neuroscience Department. I would also like to thank the University of California, Riverside School of Medicine Biomedical Sciences Program as well as my Thesis Committee for their informative comments and suggestions on this project. I would also like to thank Ken Furuichi and the staff of the UC Riverside Multidisciplinary Building vivarium for their assistance with mouse colony maintenance. I would also like to thank Dr. David Carter for training and advice on confocal microscopy. This work was done with the support of the FRAXA Foundation.

ABSTRACT OF THESIS

Evaluating Behavioral Phenotypes and FMRP Expression
in a Developmental Astrocyte-Specific Mouse Model
of Fragile X Syndrome

by

Alexandra Varallo

Master of Science, Graduate Program in Biomedical Sciences
University of California, Riverside, June 2024
Dr. Iryna Ethell, Chairperson

Fragile X Syndrome (FXS) is an inherited X-linked neurodevelopmental disorder associated with intellectual disability, sensory processing abnormalities and is one of the leading genetic causes of autism. FXS is a monogenic disorder caused by expansion of CGG repeats in the 5'-untranslated area of the Fragile X Messenger Ribonucleoprotein 1 (*FMR1*) gene, leading to a loss of its product, Fragile X Messenger Ribonucleoprotein (FMRP). Therefore, *FMR1* knock-out mice are utilized as mouse models of FXS that demonstrate similar FXS-related behavioral phenotypes, including hyperactivity and anxiety. While cell-specific mechanisms implicated in the abnormal behaviors are still under investigation, a previous study suggested that astrocytes may contribute to these deficits. In this study we tested the effects of astrocyte-specific deletion of *FMR1* gene during postnatal day (P)14-P28 developmental period on mouse behaviors. For this, we

crossed floxed *FMR1* mice with GFAP-ERT2-Cre mouse line. Astrocyte-specific *FMR1* deletion was induced in astrocytes with tamoxifen at P14 and behaviors were tested at P28. We used an open field test and elevated plus maze test to measure hyperactivity and anxiety-like behaviors. Social preference and sociability were tested using a three-chamber test. We found that these mice exhibited FXS-associated behaviors such as hyperactivity and anxiety-like behaviors in the open field with no sex differences. We also observed some differences in social preference and sociability between WT and cKO mice. Our findings suggest that timing of *FMR1* deletion from astrocytes may differentially affect neuronal activity in different brain areas, which could explain the difference in behavioral phenotypes.

TABLE OF CONTENTS

INTRODUCTION

Fragile X Syndrome

Fragile X Syndrome (FXS) is an inherited X-linked neurodevelopmental disorder associated with intellectual disability, sensory processing abnormalities and is one of the leading genetic causes of autism (Crawford, 2001). FXS is a monogenic disorder caused by expansion of CGG repeats in the 5'-untranslated area of the Fragile X Messenger Ribonucleoprotein 1 (*FMR1*) gene (Protic, 2022). Typically, healthy individuals will have 5 to 44 repeats, but individuals with FXS will have over 200 repeats (Nolin, 2006). Categories of alleles have been established: stable normal alleles have 5-44 repeats, the Gray Zone (intermediate) alleles have 45-54 repeats, Premutation alleles have 55-200 repeats with a ceiling of ~230, and the full mutations have over 230 repeats (Maddalena, 2001). The resulting CGG expansion causes an increase in methylation of the *FMR1* 5' untranslated region (Stone, 2023). The increased methylation results in silencing of the *FMR1* gene, leading to a loss of its protein product, Fragile X Messenger Ribonucleoprotein (FMRP) (Sutcliffe, 1992).

The behavioral phenotype of Fragile X Syndrome is characterized by repetitive behaviors, intellectual disability, hyperactivity, and increased anxiety (Penagarikano, 2007). Sensory processing abnormalities are also observed in FXS patients with symptoms including increased seizure susceptibility, decreased habituation to repeated auditory stimuli, and abnormal processing (Rais, 2018). In children with FXS, it is estimated that 30% of these patients also have autism (Hagerman, 2005). The estimated

prevalence of FXS varies among sexes, affecting more males than females due to being an X-linked disorder. FXS affects all major ethnic groups and is believed to affect an approximate 1:4000 males and 1:8000 females in the population (Turner, 1996). Female patients experience milder symptoms due to a compensatory mechanism by the unaffected X chromosome, and males typically exhibit stronger phenotypes compared to the females (Stone, 2023). A large proportion of female FXS patients have a healthy intellect quotient; however, approximately 60% of women with FXS have mild intellectual disability (Martorell, 2010). In a quantitative real-time polymerase chain reaction (qRT-PCR) study on human FXS patients to detect blood *FMR1* levels, male FXS patients were found to have reduced *FMR1* mRNA concentration compared to females. Additionally, when correlating FMRP concentration and *FMR1* concentration, while *FMR1* concentration and FMRP concentration were positively correlated in fully methylated DNA from *FMR1* patients, some individuals still had small amounts of FMRP despite having an *FMR1* expression that was outside the detectable amount during the assay. When correlating behaviors to *FMR1*, they observed that increased levels of *FMR1* concentration related to a higher IQ score in females, indicating that FXS patient behavior correlates with *FMR1* (Straub, 2023). In males with FXS, there are also distinct groups that express trace levels of FMRP and those completely lacking FMRP expression. In fully methylated males with FXS, they found that there is no longer a positive correlation between IQ and FMRP. Together, these findings imply that FMRP below a particular may not contribute to intellectual capacity (Boggs, 2022). Other behaviors observed in male individuals with both FXS and autism include social

avoidance, lower IQ, and lower scoring of adaptive behaviors when compared to the rest of their FXS group (Kau, 2004). By identifying the lack of *FMR1* expression from inactive X chromosomes, the findings determined that *FMR1* is a gene that is subject to X chromosome inactivation (Kirchgessner, 1995).

Fragile X Syndrome Pathology

FMRP plays a critical role in neurodevelopment and regulates messenger RNA (mRNA) transcription involves in synapse development (Protic, 2022). FXS is also characterized by hyperexcitability resulting from the loss of FMRP inducing channelopathies. Abnormalities associated with FMRP loss include changes in action potential firing through dysfunctional cation channel regulation, AMPA/NMDA receptors, and neurotransmitter release (Deng, 2021). FMRP loss leads to an imbalance of long term-depression (LTD) and long-term potentiation (LTP), resulting in deficits in synaptic plasticity (Pfeiffer, 2009). A reduction in FMRP disrupts excitation and inhibition balance in the brain through an increase in glutamate receptor expression (Protic, 2022). The absence of FMRP also results in dysregulated glutamate receptor function by upregulating mGluR-mediated long-term depression (LTD) (Ligsay, 2016). Along with a disruption in glutamate receptor activity, there is implicated dysregulation in GABAergic function and reduced inhibition in patients with FXS (D'Hulst and Kooy, 2009). $GABA_A$-receptors play a role in regulating excitation, resulting in the modulation of behaviors that are disrupted in FXS such as anxiety, cognition, and learning (Sieghart, 1999). The loss of FMRP disrupts $GABA_A$-receptor activity, resulting in a decrease in $GABA_A$-receptor-mediated tonic inhibition (Deng, 2022). Another consequence of FMRP

loss is reduced expression of GABA receptor subunits. These findings imply that FMRP potentially plays a role in the localization of GABA subunits, and decreased expression could perturb the regulation of inhibition resulting in an abnormal behavioral phenotype (D'Hulst, 2006). In a study evaluating women who are FXS premutation carriers, there are alterations in $GABA_A$-receptor activity resulting in reduced cortical and afferent inhibition (Conde, 2013). FMRP is also known to regulate synaptic transmission, and the loss of FMRP leads to structural abnormalities such as decreased dendrites and abnormal dendritic spines which could alter synaptic transmission (Salcedo-Arellano, 2020).

Frontal Cortex, Hippocampus, and Auditory Cortex in Fragile X Syndrome

The reduction in FMRP levels results in abnormal neuroanatomy in developing adolescents with FXS compared to their healthy counterparts (Sandoval, 2018). The loss of FMRP contributes to the dysfunction of the hippocampus (Bostrom, 2016). The human hippocampus is associated with complex cognitive functions such as memory formation, learning, and emotional behaviors (Deng, 2010). In the hippocampus of *FMR1* KO mice, there was an observed increase in metabotropic glutamate receptor-mediated LTD, suggesting these protein-regulated synaptic plasticity processes are disrupted (Huber, 2002). In the dentate gyrus (DG), *FMR1* KO mice exhibited increased spine density throughout development and an abundance of thin, immature spines (Grossman, 2010). Induced abnormalities of spine density in the hippocampus may also contribute to these behavioral and cognition deficits observed in FXS patients (Bostrom, 2016). The prefrontal cortex (PFC) is a brain area that processes executive function and inputs from multiple brain regions (Hathaway, 2023). In FXS, we see abnormal behavior such as

social phobia and attention deficits which are commonly associated with dysfunctions in the prefrontal cortex (Reiss, 2007). Frontal cortex morphological abnormalities associated with FXS include an increase in medial prefrontal cortex (mPFC) spine density and abnormal spine length in the *FMR1* KO compared to the WT (Liu, 2011). Similarly, in autism spectrum disorder (ASD), cortical projection neurons were found to have an abundance of dendritic spines, and this morphological change is believed to impact cortical connection (Hustler, 2010). Another symptom observed in FXS patients is enhanced cortical excitability. In EEG studies conducted on FXS patients, some abnormalities in cortical connectivity include increased gamma power and 50% of the FXS patients having gamma power levels that were significantly increased above healthy individuals. These EEG studies demonstrate that in the alpha and beta bands, there is decreased long-range functional connectivity. In contrast, in the gamma band, there is enhanced short-range connectivity (Wang, 2017). FXS patients also face difficulties habituating to repeated stimuli, and in an EEG study, these patients exhibited decreased N1 suppression when presented with repeated stimuli. This includes a reduced ERP amplitude and low-frequency phase-locking. Along with the decreased N1 response, the patients demonstrated increased gamma power along with reduced gamma phase locking, which could contribute to sensory processing abnormalities (Ethridge, 2016). These findings together verify that in FXS patients, there is increased cortical excitability and hypersensitivity.

Mouse Models of Fragile X Syndrome and Behavior Testing

The Dutch-Belgian Fragile X Consortium first introduced the *FMR1* knock-out mouse model in 1994. This mouse model is a global knock-out of *FMR1* and lacks FMRP. *FMR1* knock-out mice are utilized as mouse models of FXS that demonstrate similar FXS-related behavioral phenotypes, including hyperactivity and other neuronal alterations (THE DUTCH-BELGIAN FRAGILE X CONSORTHIUM, 1994).

Due to the aberrant behavior of the Fragile X mouse model, multiple behavior tests are used to assess anxiety-like behaviors, hyperactivity, and social impairment, which are characteristics also observed in the human model. The Open Field Test is a behavioral assessment that measures locomotor activity to verify hyperactive behaviors as well as anxiety-like behaviors. Thigmotaxis is the peripheral area of the arena closest to the surrounding walls. The Open Field is the inside of the arena that excludes thigmotaxis. Variables measured in this test include velocity in the whole arena and thigmotaxis, distance in the whole arena and thigmotaxis, and the percent time spent in the open field compared to thigmotaxis (Seibenhener, 2015). Normally mice spend more time in the thigmotaxis than in the center of the open field. Mice that show hyperactivity may run more across the open field. Another behavioral assessment for autism-like behaviors is the Elevated Plus Maze test. This test consists of a cross-shaped arena with two open arms and two closed arms surrounded by walls. The entire arena is lifted 1 meter off the ground. Variables measured in this test are the percent time spent in closed arms, % time spent in open arms, and velocity in the whole arena (Kraeuter, 2018). Mice usually prefer to spend more time in the closed arm. Another behavioral assessment to test impairments

in sociability is the Social Novelty Test. During this test, the variables measured are time spent with the stranger mouse versus the empty chamber to test for Sociability. Normally mice spend more time with the stranger mouse over the empty cup, demonstrating social motivation as indicated by Sociability. Another variable measured is the time spent with a novel mouse over a now familiar mouse to test Social Novelty Preference. Normally mice spend more time with the second stranger versus the now-familiar mouse. This behavior in normal mice is explained by the experimental mouse's social memory of the familiar mouse then demonstrating a preference for interaction with the novel subject. The time spent with Stranger 1 versus Stranger 2 provides a measurement of the preference for novelty versus familiarity in a social scenario. Overall, this assessment tests for social motivation, social memory, and preference for novelty (Kaidanovich-Beilin, 2011). Together, these are some of the tests used to assess behavioral impairments in the Global *FMR1* Knock-Out mouse model.

Role of Astrocytes

Astrocytes are glial cells that play an important role in maintaining homeostasis and regulating synaptic transmission and plasticity. Synaptic plasticity contributes to the encoding of and response to stimuli and is mediated by long-term potentiation (LTP) and long-term depression (LTD) (Yong, 2020). Glial cells are one of the major brain cell groups, and astrocytes make up a significant portion of the glial cell population (von Bartheld, 2016). Astrocytes form intercellular networks through their gap junctions, contributing to cognition and synaptic transmission (Hösli, 2022). Astrocytic glutamate transporter 1 (GLT1) is a plasma membrane transporter for glutamate, and GLT1 is

widely expressed in astrocytes to mediate glutamate homeostasis (Danbolt, 2001). GLT1 plays an important role in regulating glutamate, and a deficiency of GLT1 in astrocytes is associated with excess extracellular glutamate, contributing to neurotoxicity (Tanaka, 1997).

Astrocytic Pathologies in Fragile X Syndrome

While previous research around FXS has been primarily neuronal-focused, glial cells such as astrocytes are also an area of interest in Fragile X Syndrome. Abnormal astrocytic function is implicated in the pathology of neurodevelopmental disorders such as Fragile X Syndrome (Fernández-Blanco, 2020). Astrocytes regulate the formation of inhibitory synapse formation (Elmariah, 2005) and glutamate uptake to regulate homeostasis (Verkhratsky, 2017). In addition to maintaining support and homeostasis, disruption of astrocytes leads to dysregulation of synapse formation and transmission (Liu, 2021). The loss of astrocytic FMRP results in disrupted GLT1 and reduced glutamate uptake, leading to increased neuronal excitation observed in FXS symptomology (Higashimori, 2013). Previous research shows that a conditional astrocyte-specific deletion of *FMR1* in vivo disrupted excitatory transmission by dysregulating astrocytic GLT1 and glutamate reuptake (Higashimori, 2016). The disruption of astrocytic glutamate transporter function leads to a pathological excess of glutamate, resulting in the perturbation of excitation-inhibition balance (Schousboe, 2005). The loss of astrocytic FMRP is found to induce cortical hyperexcitability by enhancing NMDAR-mediated evoked mEPSCs (Jin, 2020).

A co-culture paradigm found that hippocampal neurons cultured with Fragile X mouse astrocytes exhibited a reduction in both pre- and postsynaptic protein aggregates and aberrant dendritic morphology compared to those cultured with wild-type astrocytes (Jacobs & Doering, 2010). In astrocyte specific *FMR1* KO mice, after 1 month of development, the mice were found to have elevated dendritic spine formation that is believed to contribute to behavioral abnormalities (Hodges, 2017). A previous co-culture study showed that WT hippocampal neurons in contact with FMRP deficient astrocytes resulted in aberrant neuronal development with increased dendritic spine formation. The same study also demonstrated that a separate culture of FXS neurons grown on WT astrocytes resulted in a partial rescue of the abnormal morphology (Jacobs, 2010). In a *FMR1* KO mouse model, there is an overabundance of long, thin dendritic spines, suggesting dysregulation of the synaptic pruning and maturation processes (Irwin, 2000).

MATERIALS AND METHODS

Mice

This project utilizes astrocyte-specific deletion of *FMR1* in mice. To achieve the developmental cell-specific deletion, we used a model generated from floxed *FMR1* mice crossed with GFAP-ERT2-Cre mice. This allows for the deletion of *FMR1* in astrocytes under the Glial Fibrillary Acidic Protein (GFAP) promoter. In this project, Wild-Type (WT) and Conditional Knock-Out (cKO) males and Heterozygous (HET) and Conditional Knock-Out (cKO) females were evaluated to assess sex differences in FMRP expression in the astrocyte specific *FMR1* deletion model. Wild-Type (WT) mice were used as a control while Heterozygous (HET) mice were used to assess the possible effects of a single allele on the resulting phenotypes. The mice were bred with WT male and cKO female or WT male and HET female pairs to achieve mixed HET, WT, and cKO litters. Prior to testing, mice were housed in an IACUC-compliant vivarium in the Multidisciplinary Research Building of the University of California, Riverside. Mice were housed with same sex littermates in up to five mice per cage. The room of the vivarium was humidity and temperature controlled with a 12-hour light/dark cycle. The mice had *ad libitum* access to food and water and were fed with standard mouse feed.

Postnatal Astrocyte-Specific Knock-Out of FMRP

From P14-P18, the mice received 0.1 mL injections of tamoxifen solution intraperitoneally for 5 consecutive days at the same time each day. The tamoxifen solution is made from 0.25 grams of tamoxifen powder in 1:9 ethanol/sunflower seed oil

solution. At P21, after the tamoxifen had been metabolized from the mice's system, the pups were weaned from their parents and housed in new cages. Mice were housed with their littermates of the same sex in up to five mice per cage. After weaning, mice were anesthetized under an isoflurane and oxygen mixture and received numbered ear tags for identification. While still under anesthesia, tail tissue was collected and immediately placed on ice for genotyping through a third-party organization, Transnetyx, to confirm the genetic knock-out. Following tail tissue collection, the mouse's tail was coated in veterinary-grade coagulant at the wound site to stop the bleeding. The mouse was returned to the home cage and undisturbed to allow for recovery.

Behavior Testing and Tissue Collection

Prior to behavior testing, mice were housed in an IACUC-compliant vivarium with same sex littermates up to 5 mice per cage. Behavior testing was performed at P27-P29, and brains were collected the day of behavior testing. On testing days, mice would be tested for behavior between 7 AM and 2 PM. Prior to testing, cages would be brought from the vivarium to the behavior testing room, and the mice habituated in their home cage for 30 minutes in the behavior room prior to behavior testing. Mice were tested individually in each arena then placed in a cage separate from mice that have not yet undergone testing to prevent biasing results. Following behavior testing, mice were euthanized with isoflurane and was confirmed by toe pinches with increased pressure. Female mice used for tissue collection but not used for histochemical analysis and were euthanized with isoflurane. Euthanasia was confirmed with cervical dislocation. Brains without td-Tomato were collected after behavior for immunohistochemical analysis of FMRP levels, GS

expression, and DAPI expression, and brains with td-Tomato were collected to assess astrocytic expression.

Experimental Groups for Analysis

The experimental groups evaluated in this study were WT males, HET females, and astrocyte-specific cKO males and females. When WT males and HET females were observed to have similar behavioral phenotypes, these groups were combined for the Two-Way ANOVA analysis of behavior testing. When assigning experimental groups, the cKO were further divided into two groups for analysis based on level of Cre expression. Cre expression was given as a numerical value through Transnetyx genotyping. Astrocytic cKO mice with High Cre signal were designated as the cKO group, while cKO mice with Low Cre signal were found to express WT-like behavioral phenotypes and were categorized as a separate cKO group. The level of Cre expression was divided by having a Cre signal of 1 – 5 be defined as the Low Cre cKO group and a Cre signal of 5 – 10 be defined as the High Cre cKO group. The Low Cre cKO group has 1 copy of Cre while the High Cre cKO group has 2 copies of Cre.

Behavioral Testing

Open Field Test

Anxiety-related behavior and locomotive activity was measured using the Open Field Test in the cKO mice. This test would serve as the first test in the behavioral test battery for the cKO mice and the mice did behavior testing between 7 AM and 2 PM. Prior to testing, the cages were moved to the experimental room for habituation 30 minutes before

the behavior testing began. The mice always performed the Open Field Test before Elevated Plus Maze. The open field arena had a base made of a single opaque transparent sheet, and the walls consisted of acrylic sheets completely covered in white paper. The arena was a 72 x 72 cm size and stood at 50 cm tall. The arena is placed in a brightly lit room. The mice were allowed to freely explore the open field arena for 10 minutes while being digitally recorded from above the arena using the software iSpy. Before and after testing and between each mouse, the floor of the maze was cleaned with 3% acetic acid, 70% ethanol, and water to eliminate odor trails and to clean urine and fecal matter. For the analysis, the software TopScan Lite (Clever Sys., Inc., VA) was used (RRID:SCR_014494). When defining the areas of the arena, the base of the arena was divided into a 4x4 grid. The outer squares then had the outer 4 cm of the square sectioned off to be defined as the area measuring thigmotaxis during the test. The center of the middle 4 squares in this grid was defined to be the center of the arena. When creating the arena for analysis in TopScan Lite (RRID:SCR_014494), the regions of the square were defined by proximity to the center and analysis was done for each of these areas individually and the whole arena. The mouse was recorded for 10 minutes uninterrupted, and the analysis was done for the first 5-minute interval, the last 5-minute interval, and the entire 10-minute period. During the testing and analysis, the experimenter was blind to the condition of the test. The distance and velocity traveled in the entire arena was analyzed as well as the tendency for the mouse to remain in thigmotaxis. These were proxy measures for anxiety. The software GraphPad Prism 10 was used to perform statistical analysis on the parameters of interest (RRID:SCR_002798).

Elevated Plus Maze

The Elevated Plus Maze is an elevated arena with 4 arms forming a plus arrangement. This test would serve as the second test in the behavioral test battery for the cKO mice and the mice did behavior testing between 7 AM and 2 PM. This test was always performed after the Open Field Test and before the Social Novelty Test. Each of the arms was 10 cm wide x 30 cm long, and the entire arena was elevated 1 meter off the ground. Two opposing arms do not have walls (defined as open arms) and the other two opposing arms had 15 cm tall walls (defined as closed arms). During analysis, the very center of the maze where the arms converged was defined in the closed arm segment. The mice freely explored the arena for 10 minutes while being digitally recorded from above the arena with the software iSpy. Before and after testing and between each experimental mouse, the floor of the maze was cleaned with 3% acetic acid, 70% ethanol, and water to eliminate odor trails and to clean urine and fecal matter. Throughout the duration of the experiment, the experimenter was seated behind a black screen to prevent being seen by the experimental mice. The analysis was performed using TopScan Lite (Clever Sys., Inc., VA) (RRID:SCR_014494). The mouse was recorded for 10 minutes, and analysis was performed for the first 5-minute period, the second 5-minute period, and the entire 10-minute period. During the testing and analysis, the experimenter was blind to the condition of the test. When creating the arena for analysis on TopScan Lite (RRID:SCR_014494), the closed arms were defined as the parts of the arena enclosed by the walls and the center of the arena where all 4 arms converge. The open arms were defined only as the arms that didn't have the wall. The distance and velocity traveled in

the both the open and closed arms was analyzed as well as the numbers of bouts between the open and closed arms. Locomotive activity was measured using the amount of distance traveled in the entire arena, the velocity in the entire arena, and the number of bouts between the open and closed arms. The amount of time spent in the open versus the closed arms was used as a measure for anxiety in the test subjects. The software GraphPad Prism 10 was used to perform statistical analysis of the data collected on the parameters of interest (RRID:SCR_002798).

Social Novelty Test

The Social Novelty Test was used to assay sociability and social memory with novel mice. This test would serve as the third test in the behavioral test battery for the cKO mice and the mice did behavior testing between 7 AM and 2 PM. This test was always performed last following the Elevated Plus Maze. The arena used for the test was a rectangular box made of Plexiglas. The rectangular box contained three adjacent chambers of the same size, 19 cm x 45 cm. The walls of the chambers are 30 cm in height. The transparent outer walls of the Plexiglas were covered with white paper while the bottom of the arena was transparent. The left and right chambers are separated from the middle chamber by a removable divider wall. Removal of these divider walls would allow the test subject to freely roam all three chambers. Inside both the left and right chambers, there is a wire cup. At the beginning of the test, the experimental mouse is placed in the middle chamber with the divider walls preventing access to the left and right chambers. The mouse is allowed to habituate for 5 minutes in the middle chamber before the start of the tests. In the first session, a second mouse (Stranger 1 (S1)) is

placed into one of the wire cups in the left or right chamber. The chamber that would hold S1 is randomly determined and changed between the trials of experimental mice. The wire cup in the opposite chamber would remain empty for the first session. The divider walls are removed, and the experimental mouse is allowed to explore the three chambers for 10 minutes. During this time, the mouse is digitally recorded from above using the software iSpy. During the second session, a second new mouse (Stranger 2 (S2)) is placed in the empty wire cup in the opposite side of the Stranger 1 chamber. For the second session, Stranger 1 is defined as the familiar mouse and remains in its original chamber while Stranger 2 is defined as the novel mouse. The experimental mouse is allowed to freely explore the three chambers for 10 minutes. During this time, the mouse is digitally recorded from above using the software iSpy. Before and after testing and between each mouse, the floor of the maze was cleaned with 3% acetic acid, 70% ethanol, and water to eliminate odor trails and to clean urine and fecal matter. The experimenter was seated behind a black screen to prevent being seen by the experimental mice. For the analysis, the software TopScan Lite (Clever Sys., Inc., VA) was used (RRID:SCR_014494). When creating the digital arena to perform the analysis, the first and second 10-minute sessions are analyzed separately. In the first session, the middle chamber is defined as the Habituation Zone, the chamber containing Stranger 1 is defined as S1 Zone, and the chamber with the empty wire cup is defined as the Empty Zone. The area surrounding the wire cup on both the S1 chamber and the empty chamber is defined as “S1 Close” and “Empty Close” to differentiate the area closest to the wire cups that would indicate interaction. In the second session, the middle chamber is defined as the Habituation Zone,

the chamber containing Stranger 1 is defined as S1 Zone, and the chamber containing Stranger 2 is defined as the S2 zone. The area surrounding the wire cup on both the S1 chamber and the S2 chamber is defined as “S1 Close” and “S2 Close” to differentiate the area closest to the wire cups that would indicate interaction. During the analysis, the mouse was tracked by the position of its nose, and the time spent in Empty Close, S1 Close, and S2 Close was considered for the calculations made in the analysis. In the first session, the parameters measured are the duration and percentage of time spent in the Habituation Zone, S1 Zone, and Empty Zone. The sociability index is calculated by (Time in S1 Chamber/ (Time in S1 Chamber + Time in Empty Chamber)). This is used to determine the preference of the experimental mouse to be with the stranger mouse over the habituation chamber and the empty chamber. If the value of the sociability index is > 0.5, this indicates that the experimental mouse spends more time in the S1 chamber compared to the empty chamber. If the value of the sociability index is < 0.5, this indicates that the experimental mouse spends more time in the empty chamber compared to the S1 chamber. If the value of the sociability index is 0.5, this indicates that the experimental mouse spends an equal amount of time in the S1 and empty chambers. A social novelty preference index is calculated by (Time in S2 Chamber/ (Time in S1 Chamber + Time in S2 Chamber)). This is used to determine the preference of the experimental mouse to be with the novel mouse over the now familiar mouse. If the value of the social novelty preference index is > 0.5, this indicates that the experimental mouse spends more time in the S2 chamber compared to the S1 chamber. If the value of the social novelty preference index is < 0.5, this indicates that the experimental mouse

spends more time in the S1 chamber compared to the S2 chamber. If the value of the social novelty preference index is 0.5, this indicates the experimental mouse spends an equal amount of time in the S2 and S1 chambers. The software GraphPad Prism 10 was used to perform statistical analysis of the data collected on the parameters of interest (RRID:SCR_002798).

Tissue Collection

Transcardial Perfusions

Tissue was collected from mice during P27 – P29 immediately following behavior testing. Mice were euthanized using isoflurane administration in a glass jar. Three toe pinches on each foot were used to confirm euthanasia. Transcardial perfusion was performed with 30 mL of ice cold 1X Phosphate-buffered saline (PBS) to flush blood from the circulatory system. This was followed by transcardial perfusion with 30 mL of 4% paraformaldehyde (PFA) to fix the brain. Following the perfusion, the brain was dissected then fixed for an additional 2 hours in 5 mL of ice cold 4% PFA and stored in a 4-degree Fahrenheit refrigerator for the post-fixing process. After fixing with PFA, the brain was stored in a foil-covered tube containing 1X PBS. The tissue was stored in PBS in a 4-degree Fahrenheit refrigerator prior to immunostaining.

Brain Slicing

Prior to brain slicing, brains were stored at 4 degrees Celsius in 1x PBS and covered in foil. For the FMRP and GS co-stained sample image, brains were sliced into 100 μm slices using a vibratome. The brains were embedded in 8% agarose and left to harden

before being mounted on the vibratome. Slicing took place in 1X PBS solution, and slices were carefully handled with a thin paintbrush and stored in a well plate filled with PBS before staining and mounting.

For FMRP staining alone protocol, brains were also sliced into 50 μm slices using a cryostat. Prior to slicing, brains underwent a 1-hour post-fix in 4% PFA following dissection. After the post-fix, the brains were transferred to a 30% sucrose solution and given 24 hours for the brain to sink. After the brains sink, the brains were flash-frozen in isopentane on dry ice then stores in -80-degree Celsius until slicing. Slices collected from the cryostat were transferred to a well plate containing fresh PBS and then placed in a 4-degree refrigerator for short-term storage until staining.

Immunohistochemistry

Immunohistochemistry was performed to stain for Fragile X Messenger Ribonucleoprotein (FMRP). 50 and 100 μm slices containing frontal cortex (FC), hippocampus (HPC), and auditory cortex (AuC) were used in the stain. Each wash would be 200 μL per well for blocking buffer and antibodies, and washes with PBS, PFA, and Phosphate-Buffered Saline with Triton-X (PBST) will be performed with 500 μL per well. Immunohistochemistry was performed with free floating slices in a well plate at room temperature in a dim room. Photo-sensitive steps of the stain would take place with the well-plate covered in foil to protect the samples from exposure to ambient light in the histology room. Antibodies used in the staining process will be diluted in PBST. Washes and incubation with permeabilization buffer were performed with 1X PBST buffer made

from 1X PBS with 0.5% Triton-X 100. The slices are first incubated with blocking buffer made from 10% goat serum with 1 drop of Avidin per 2 mL in PBST for an hour. Following this step, the slices would be incubated with a Biotin PBST block made from 1 drop Biotin per 4 mL of PBST for 15 minutes at room temperature. Following this step, the slices were incubated with primary antibody (Mouse anti-FMRP) at a 1:1000 dilution for 48 hours at 4 degrees Celsius. After the incubation, the slices would be washed with PBST at room temperature then incubated with the secondary antibody (Goat anti-Mouse Biotin) at a 1:1000 dilution overnight at 4 degrees Celsius while wrapped in aluminum foil. After this incubation, the slices would be incubated with Streptavidin Cy5 at a 1:1000 dilution for 2 hours at room temperature. The slices are then washed with PBST and PBS at room temperature. After the washes following secondary antibody incubation, the slices are mounted onto charged slides with mounting media with DAPI. The stained slides are stored in containers to prevent light exposure in a 4 degrees Celsius refrigerator. Immunohistochemistry was always performed with fresh solutions made the day of experimentation.

Immunohistochemistry was also used to perform a co-stain for glutamate synthase (GS) and FMRP as seen in the sample image of a P28 KO mouse hippocampus. To achieve this co-stain, the slices were post-fixed, stained for FMRP, post-fixed, stained for GS, then mounted. Slices were sliced on the vibratome into 100 μm slices and washed in a well plate with two slices per well. Each wash would be 200 μL per well for blocking buffer and antibodies, and washes with PBS, PFA, and Phosphate-Buffered Saline with Triton-X (PBST) will be performed with 500 μL per well. Immunohistochemistry was performed

at room temperature in a dim room. Photo-sensitive steps of the stain would take place with the well-plate covered in foil to protect the samples from exposure to ambient light in the histology room. Antibodies used in the staining process will be diluted in PBST. Prior to staining, slices were post-fixed on ice in 4% PFA for 30 minutes. Washes and incubation with permeabilization buffer were performed with 1X PBST buffer made from 1X PBS with 0.5% Triton-X 100. The slices were incubated with Biotin PBST block. Following the block, the slices were incubated with the primary antibody (Mouse anti-FMRP) at a 1:200 dilution for 48 hours at 4 degrees Celsius. After primary antibody incubation, the slices would undergo incubation with the secondary antibody (Goat anti-FMRP) at a 1:200 dilution overnight, and the well-plate will be covered with aluminum foil. The following day, the slices will be incubated with Streptavidin Cy5 at a 1:200 dilution for 2 hours. Following the washes after the Streptavidin incubation, the slices would undergo a second post-fix in PFA on ice for 30 minutes to prepare for the GS stain. During the second-post fix, the plate was covered in foil to protect the slices from ambient light. The slices were incubated with permeabilization buffer for 30 minutes then incubated with blocking buffer for 1 hour at room temperature in the dark. After the blocking buffer, the slices are incubated with primary antibody (Anti-GS (Rabbit)) at a 1:500 dilution at 4 degrees Celsius overnight. The following day, the slices will be incubated with secondary antibody (Donkey anti-Rabbit) at a 1:500 dilution at room temperature for 2 hours. After the washes following secondary antibody incubation, the slices are mounted onto charged slides with mounting media with DAPI. The stained

slides are stored in containers to prevent light exposure in a 4 degrees Celsius refrigerator. Immunohistochemistry was performed with fresh solutions.

Confocal Microscopy

Images of the brain slices were taken using a confocal Zeiss 880 Inverted Microscope. Confocal images were taken with coronal slices from the frontal, middle, and caudal sections of the brain. The frontal slices contained frontal cortex (FC), the middle slices contained CA1 hippocampus (HPC), and auditory cortex (AuC). Images of td-Tomato astrocytic expression and FMRP expression were captured with 5x objectives for tiled slice images and 20x objectives for representation of specific brain areas. Tiles images were taken at 5x and included stacks of 10 μm thickness. These tiled images were taken to give a representative image of the brain slices and areas we further examined. Images taken at 20x were taken with z-stacks of 2 μm intervals with a stack thickness of 10 μm. Images were acquired under identical conditions, and each slide corresponding to an animal contained 2 slices from each brain region. For the representative image taken with the FMRP, GS, and DAPI stain, this image was acquired with 20x objectives. These representative images were taken with a z-stack of 2 μm intervals with a stack thickness of 10 μm. The image was saved as a .tif file, and I proceeded to compress the z-stack, make a composite image, and brighten the colors. The program used to compress the composite image and make adjustments was ImageJ (Schindelin, 2012).

Statistical Analysis

Statistical analysis of behavior was conducted using GraphPad Prism 10 (RRID:SCR_002798). The first comparisons made were between the WT males and KO males and then between the HET females and KO females. This data was analyzed with an unpaired t-test, and the data represents the mean and standard error of the mean (SEM). A Two-Way ANOVA followed by a Tukey multiple-comparison post-test was performed to assess potential sex and genotype interactions in the Open Field Test, Elevated Plus Maze Test, and Social Novelty Test. However, the Two-Way ANOVA demonstrated there were significant interactions with genotype-based differences but not for sex differences or sex x genotype interactions for the KO. For further analysis, a One-Way ANOVA followed by a Tukey multiple-comparison post-test was performed to compare genotype differences. Due to the lack of sex differences observed by the Two-Way ANOVA followed by Tukey multiple-comparison post-test, the male and female cKO groups were combined to create an overall cKO group to compensate for a smaller n value in the individual groups. This would allow for a robust, comparable n value to the WT and HET groups and more comparable numbers across the different genotype groups. In the One-Way ANOVA, we compared WT males, HET females, the low Cre cKO group and the combined High Cre cKO group in all 3 tests.

RESULTS

Cre Signal Distribution in the cKO Groups

Cre signal is one of the variables used to determine the experimental groups. The Cre signal was provided as a numerical value through Transnetyx and was measured in the Conditional Knock-Out in both the Male and Female groups. The Knock-Out group for both sexes was further divided into a High Cre cKO and Low Cre cKO group. In both the Male and Female group, there is a significant difference between the High Cre cKO group and the Low Cre cKO group with the High Cre cKO group having a greater Cre signal (Figure 1).

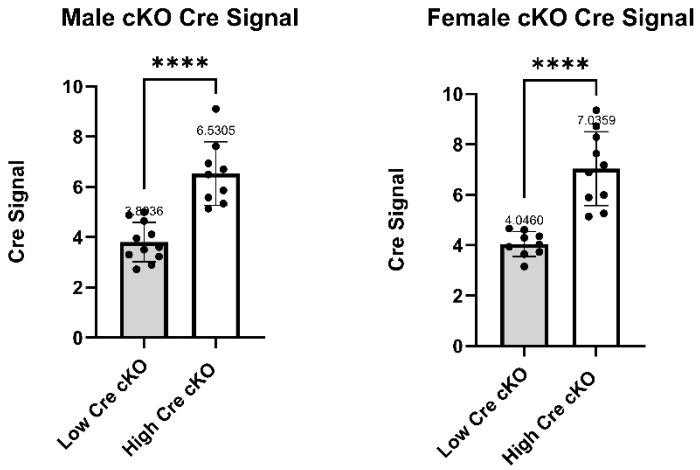

Figure 1. Graphs show Cre signal in the Low Cre cKO and the High Cre cKO for the males and females. A substantial difference in Cre signal is observed between the Low Cre cKO and the High Cre cKO group in both the Males and Females. (Male High Cre cKO n = 9, Male Low Cre cKO n = 11, Female High Cre cKO n = 10, Female Low Cre cKO n = 9; *P < 0.05; **P < 0.01; ***P < 0.001; ****P < 0.0001; t-test).

Open Field Test

Measurements of hyperactivity were evaluated in the Open Field Test. One variable considered is Distance in the Whole Arena. To evaluate potential sex differences, the cKO was compared to the WT and HET groups in the males and females. In the Male Group, during the 5 – 10 min time interval and whole 10 min intervals, the cKO group traveled more distance compared to the WT group. However, this difference was not observed in the 0 – 5 min interval (Figure 2A). In the Female Group, differences were observed in the 0 – 5 min, 5 – 10 min, and the whole 10 min intervals. The cKO group traveled more distance compared to the HET group at all time points (Figure 2B). Differences were also assessed across the different genotypes. During the 0 – 5 min interval, the High Cre cKO traveled a more distance compared to the HET group. During the 5 – 10 min interval, the High Cre cKO also traveled more distance compared to the WT, HET, and Low Cre cKO group. However, there were no differences between the WT, HET, and Low Cre cKO groups (Figure 3).

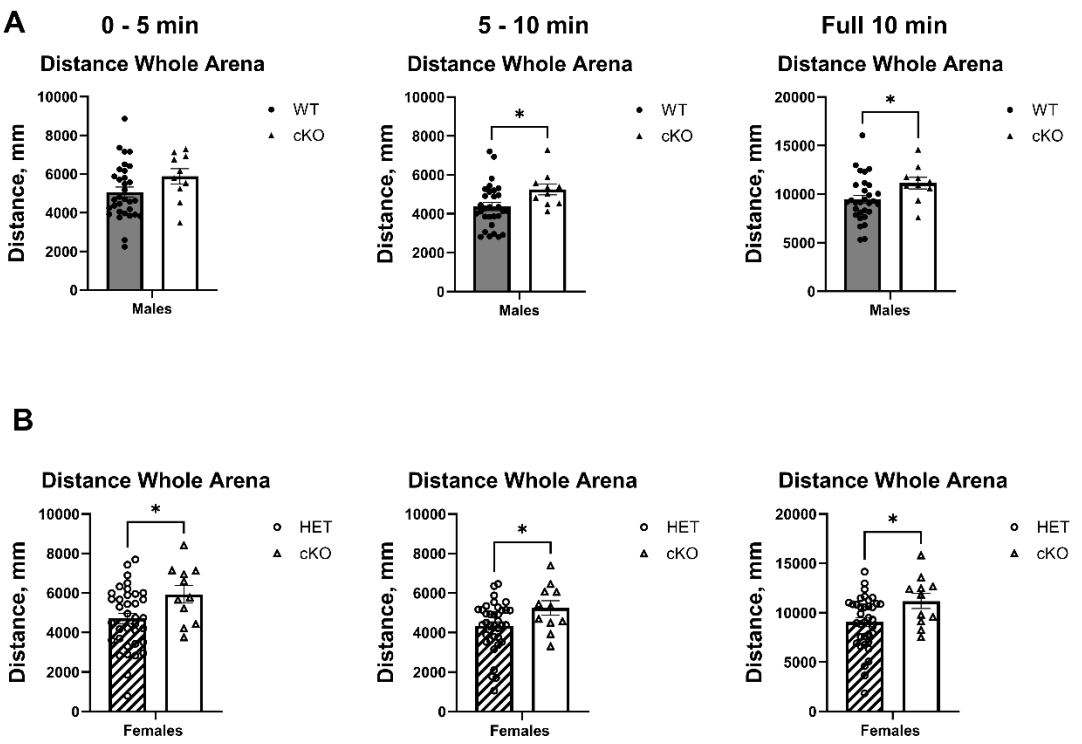

Figure 2. (A-B) Graphs describe measurements of hyperactivity in the Open Field Test (OFT). A. Distance in Whole Arena in the Open Field in Males. Observed differences between WT and cKO (High Cre cKO) group in 5 – 10 min and full 10 min intervals. cKO demonstrated increased hyperactivity compared to the WT. No differences were observed in the 0 – 5 min interval. B. Distance in Thigmotaxis in the Open Field in Females. Observed differences between HET and cKO at all time points. cKO demonstrated increased distance traveled in the whole arena compared to WT (WT n = 29, HET n = 34, Male cKO n = 9, Female cKO n = 11; *P < 0.05; t-test).

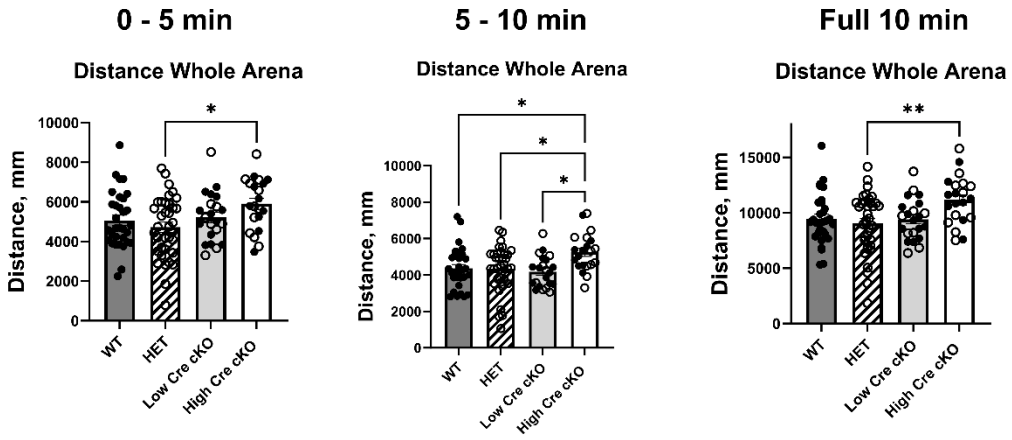

Figure 3. Graphs describe measurements of hyperactivity in the Open Field Test (OFT). Observed differences between the Heterozygous females and the High Cre cKO group in 0 – 5 min interval. The High Cre cKO group demonstrated increased hyperactivity compared to the HET group. Observed differences between the WT and the High Cre cKO, the HET and the High Cre cKO, and the Low Cre cKO and the High Cre cKO. The High Cre cKO group demonstrated increased hyperactivity compared to all 3 other groups in the 5 – 10 min interval of the test. Overall, in the full 10 min duration of the task, there were differences between the HET and the High Cre cKO (WT n = 29, HET n = 34, Male High Cre cKO n = 9, Female High Cre cKO n = 11; Male Low Cre cKO n = 9, Female Low Cre cKO n = 9; *P < 0.05; **P < 0.01; One-Way ANOVA followed by Tukey multiple-comparison post-test).

Measurements of hyperactivity were evaluated in the Open Field Test. Another variable considered is Distance in Thigmotaxis. To evaluate potential sex differences, the cKO was compared to the WT and HET groups in the males and females. In the Male Group, during the 0 – 5 min time interval and whole 10 min intervals, the cKO group traveled more distance compared to the WT group. However, this difference was not observed in the 5 – 10 min interval (Figure 4A). In the Female Group, differences were observed in the 0 – 5 min interval. However, this difference was not observed in the 5 – 10 min or full 10 min interval. The cKO group traveled more distance in thigmotaxis compared to the HET group in the 0 – 5 min interval (Figure 4B). Differences were also assessed across the different genotypes. There were no differences observed between the WT, HET, Low Cre cKO, and High Cre cKO at any of the time intervals. This indicates no significant difference in this measure of hyperactivity across genotypes (Figure 5).

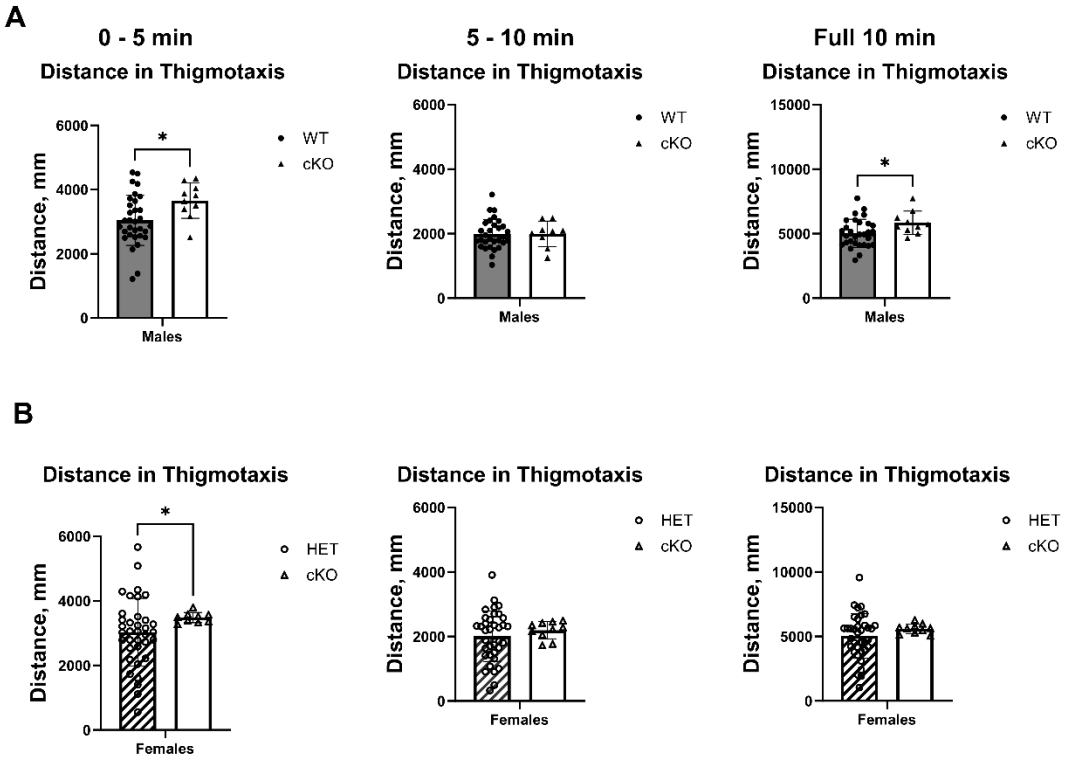

Figure 4. (A-B) Graphs describe measurements of hyperactivity in the Open Field Test (OFT). A. Distance in Thigmotaxis in Males. Observed differences between WT and cKO (High Cre cKO) group in the 0 – 5 min and full 10 min intervals. cKO demonstrated increased hyperactivity compared to the WT. No differences were observed in the 5 – 10 min interval. B. Distance in Thigmotaxis in Females. Observed differences between HET and cKO in the 0 – 5 min interval but not the 5 – 10 or full 10 min intervals. The cKO demonstrated increased distance traveled in the whole arena compared to HET (WT n = 29, HET n = 34, Male cKO n = 9, Female cKO n = 11; *P < 0.05; t-test).

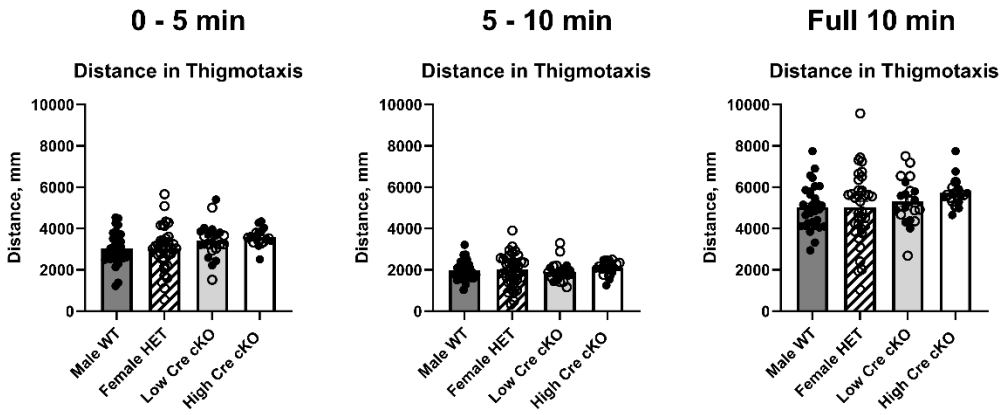

Figure 5. Graphs describe measurements of hyperactivity in the Open Field Test (OFT). A. Distance in Thigmotaxis in the Open Field in Males. Observed no differences between groups in the 0 – 5 min, 5 – 10 min, and full 10 min intervals. Indicates no significant differences in this measure of hyperactivity between the different genotypes (WT n = 29, HET n = 34, Male High Cre cKO n = 9, Female High Cre cKO n = 11; Male Low Cre cKO n = 9, Female Low Cre cKO n = 9; One-Way ANOVA followed by Tukey multiple-comparison post-test).

Measurements of hyperactivity were evaluated in the Open Field Test. Another variable considered is Velocity in the Whole Arena. To evaluate potential sex differences, the cKO was compared to the WT and HET groups in the males and females. In the Male Group, during the 5 – 10 min time and whole 10 min intervals, the cKO group traveled at a higher velocity compared to the WT group. However, this difference was not observed in the 0 – 5 min interval (Figure 6A). In the Female Group, differences were observed in the 0 – 5 min, 5 – 10 min, and the full 10 min intervals. The cKO group traveled at a higher velocity compared to the HET group at all time points (Figure 6B). Differences were also assessed across the different genotypes. During the 0 – 5 min interval, the High Cre cKO traveled at a higher velocity compared to the HET group. During the 5 – 10 min interval, the High Cre cKO traveled at a higher velocity compared to the WT, HET, and Low Cre cKO group. However, there were no differences between the WT, HET, and Low Cre cKO groups. In the full 10 min interval, the High Cre cKO travels at a higher velocity than the HET group (Figure 7).

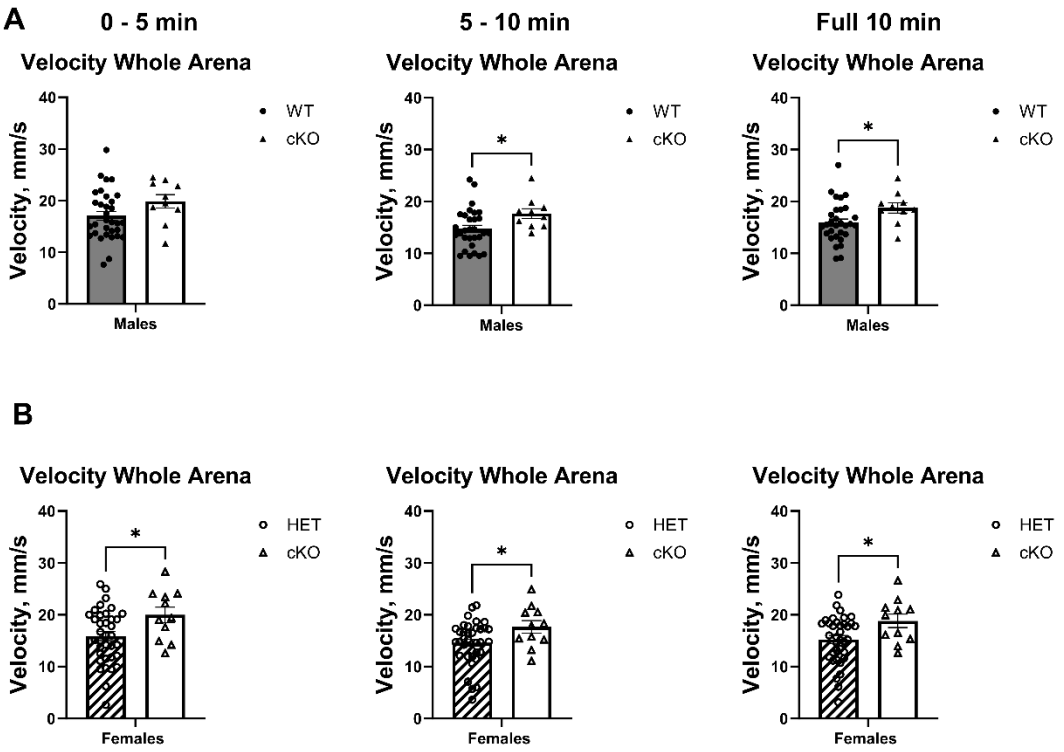

Figure 6. (A-B) Graphs describe measurements of hyperactivity in the Open Field Test (OFT). A. Velocity in the Open Field in Males. Observed differences between WT and cKO group in the 5 – 10 min and full 10 min interval. The cKO demonstrated increased hyperactivity compared to the WT. B. Velocity in the Open Field in Females. Observed differences between HET and cKO at all time intervals. The cKO demonstrated increased hyperactivity compared to the HET (WT n = 29, HET n = 34, Male cKO n = 9, Female cKO n = 11; *P < 0.05; t-test).

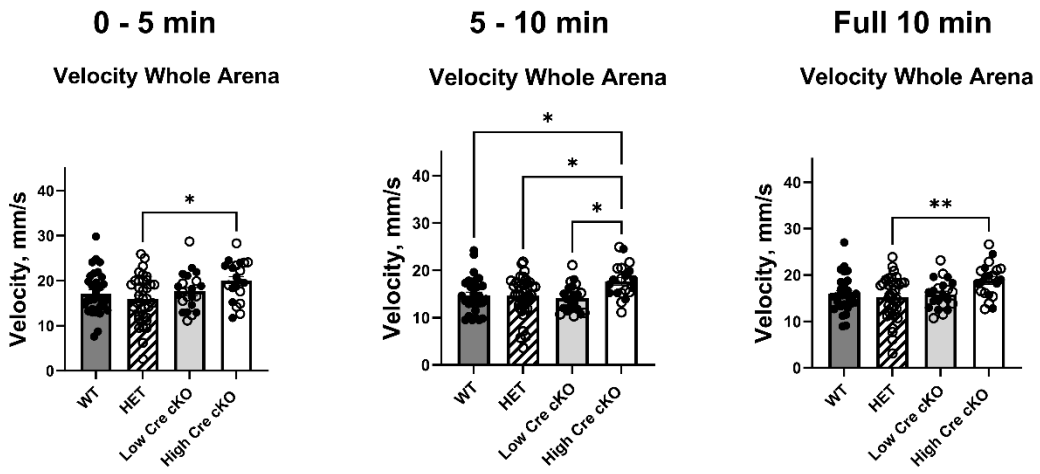

Figure 7. Graphs describe measurements of hyperactivity in the Open Field Test (OFT). Observed differences between the HET and High Cre cKO during the 0 – 5 min interval. The High Cre cKO demonstrated increased hyperactivity compared to the HET. Observed differences between the WT and the High Cre cKO, the HET and the High Cre cKO, and the Low Cre cKO and the High Cre cKO. The High Cre cKO group demonstrated increased hyperactivity compared to all 3 other groups in the 5 – 10 min interval. Overall, in the full 10 min interval, there were differences between the HET and the High Cre cKO. The High Cre cKO demonstrated increased hyperactivity compared to the HET (WT n = 29, HET n = 34, Male High Cre cKO n = 9, Female High Cre cKO n = 11; Male Low Cre cKO n = 9, Female Low Cre cKO n = 9; *P < 0.05; **P < 0.01; One-Way ANOVA followed by Tukey multiple-comparison post-test).

Measurements of hyperactivity were evaluated in the Open Field Test. Another variable considered is Velocity in Thigmotaxis. To evaluate potential sex differences, the cKO was compared to the WT and HET groups in the males and females. In the Male Group, during the 5 – 10 min and full 10 min intervals, the cKO group traveled at a higher velocity compared to the WT group. However, this difference was not observed in the 0 – 5 min interval (Figure 8A). In the Female Group, differences were observed in the 0 – 5 min, 5 – 10 min, and the full 10 min intervals. The cKO group traveled at a higher velocity compared to the HET group at all time points (Figure 8B). Differences were also assessed across the different genotypes. During the 0 – 5 min interval, the High Cre cKO traveled at a higher velocity compared to both the HET and WT group. During the 5 – 10 min interval, the High Cre cKO traveled at a higher velocity compared to the WT, HET, and Low Cre cKO group. However, there were no differences between the WT, HET, and Low Cre cKO groups. In the full 10 min interval, the High Cre KO travels at a higher velocity than the WT, HET, and Low Cre cKO group (Figure 9).

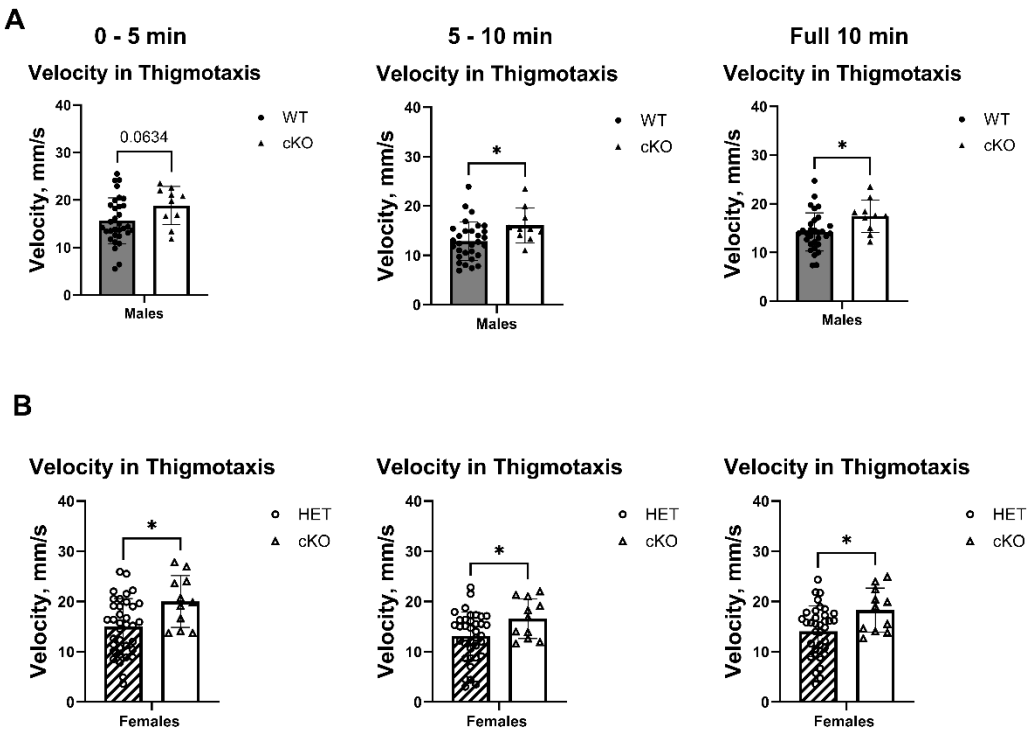

Figure 8. (A-B) Graphs describe measurements of hyperactivity in Thigmotaxis. A. Velocity in Thigmotaxis in Males. Observed differences between WT and cKO group in the 5 – 10 min and full 10 min intervals. The cKO demonstrated increased hyperactivity compared to the WT. B. Velocity in the Thigmotaxis in Females. Observed differences between HET and cKO at all time intervals. The cKO demonstrated increased hyperactivity compared to the HET (WT n = 29, HET n = 34, Male cKO n = 9, Female cKO n = 11; *P < 0.05; t-test).

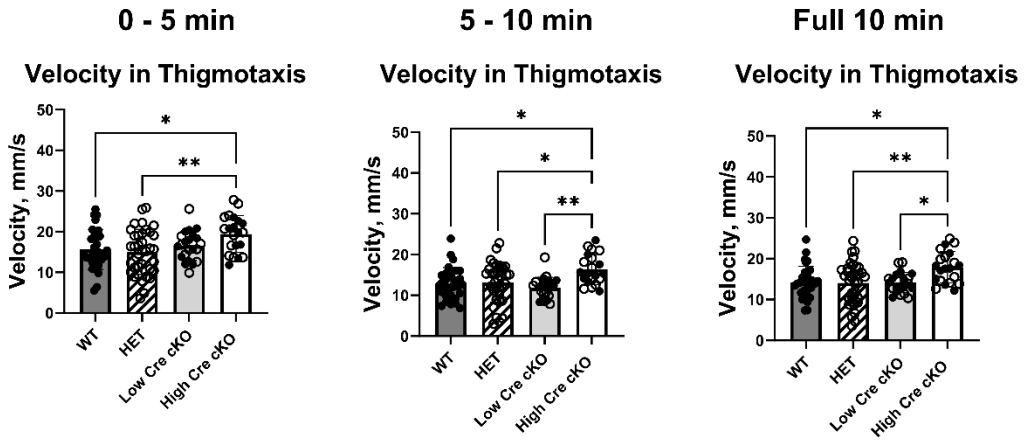

Figure 9. Graphs describe measurements of hyperactivity in Thigmotaxis. Observed differences between WT and High Cre cKO groups in the 0 – 5 min, 5 – 10 min, and full 10 min intervals. The High Cre cKO demonstrated increased hyperactivity compared to the WT. Observed differences between HET and High Cre cKO groups in the 0 – 5 min, 5 – 10 min, and the full 10 min intervals. The High Cre cKO demonstrated increased hyperactivity compared to the HET. Observed differences between the Low Cre cKO and the High Cre cKO groups in the 5 – 10 min and full 10 min intervals but not the 0 – 5 min interval (WT n = 29, HET n = 34, Male High Cre cKO n = 9, Female High Cre cKO n = 11; Male Low Cre cKO n = 9, Female Low Cre cKO n = 9; *P < 0.05; **P < 0.01; One-Way ANOVA followed by Tukey multiple-comparison post-test).

Measurements of anxiety-like behaviors were evaluated in the Open Field Test. Another variable considered is % Time Spent in the Open Field. To evaluate potential sex differences, the cKO was compared to the WT and HET groups in the males and females. In the Male Group, during the 5 – 10 min time interval, the cKO group spent more time in the Open Field compared to the WT group. However, this difference was not observed in the 0 – 5 min or in the full 10 min intervals (Figure 10A). In the Female Group, no differences were observed in the 0 – 5 min, 5 – 10 min, or the full 10 min intervals (Figure 10B). Differences were also assessed across the different genotypes. There were no observed differences were observed in the 0 – 5 min, 5 – 10 min, or the full 10 min intervals (Figure 11).

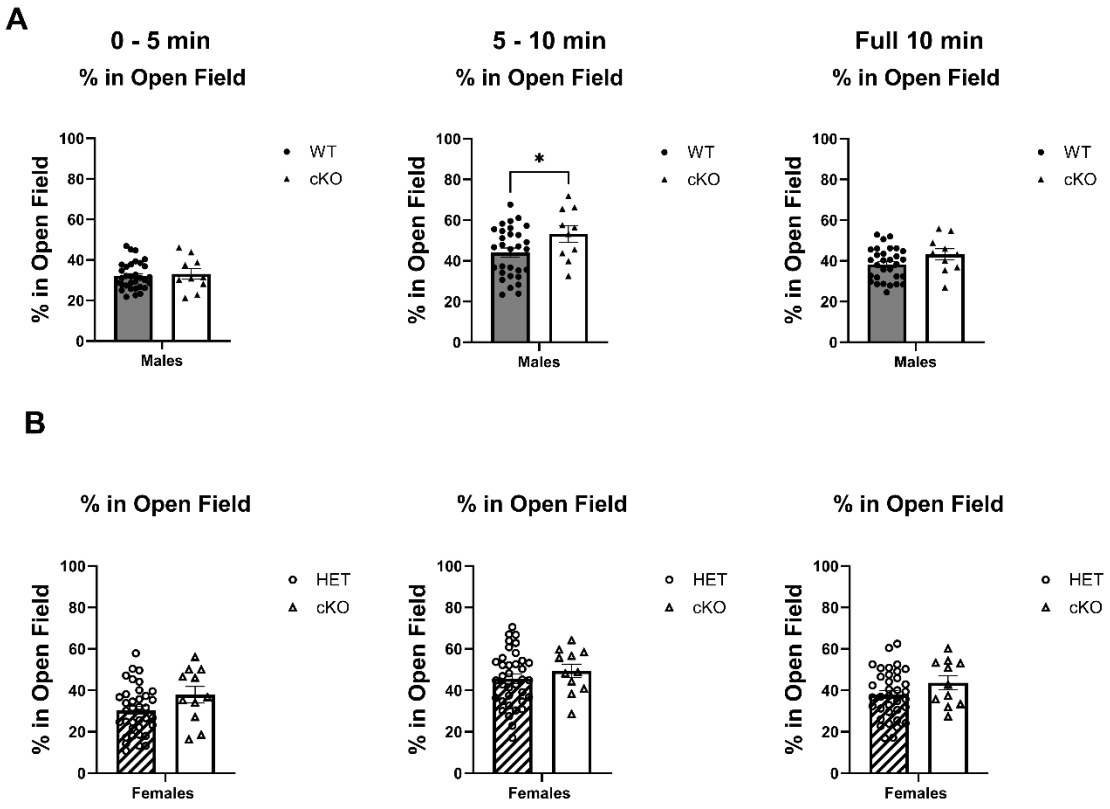

Figure 10. (A-B) Graphs describe anxiety-like behaviors in the Open Field Test (OFT). A. Percent time spent in Open Field in Males. Observed no differences between WT and cKO group in the 0 – 5 min or the full 10 min intervals. Observed cKO spent more time in Open Field in 5 – 10 min interval. B. Percent time spent in Open Field in Females. Observed no differences within the 0 – 5 min, 5 – 10 min, or the full 10 min intervals (WT n = 29, HET n = 34, Male cKO n = 9, Female cKO n = 11; *P < 0.05; t-test).

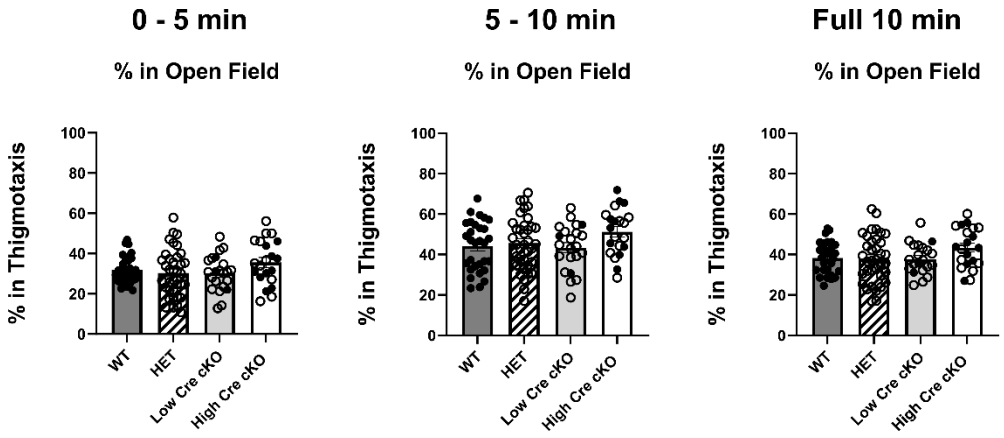

Figure 11. Graphs describe anxiety-like behaviors in the Open Field Test (OFT). Observed no differences between groups within the 0 – 5 min, 5 – 10 min, or the full 10 min intervals. Indicates no significant differences in anxiety-like behaviors between the different genotypes (WT n = 29, HET n = 34, Male High Cre cKO n = 9, Female High Cre cKO n = 11; Male Low Cre cKO n = 9, Female Low Cre cKO n = 9; One-Way ANOVA followed by Tukey multiple-comparison post-test).

Measurements of anxiety-like behaviors were evaluated in the Open Field Test. Another variable considered is % Time Spent in Thigmotaxis. To evaluate potential sex differences, the cKO was compared to the WT and HET groups in the males and females. In the Male Group, no differences were observed in the 0 – 5 min, 5 – 10 min, or the full 10 min intervals (Figure 12A). In the Female Group, no differences were observed in the 0 – 5 min, 5 – 10 min, or the full 10 min intervals (Figure 12B). Differences were also assessed across the different genotypes. There were no observed differences were observed in the 0 – 5 min, 5 – 10 min, or the full 10 min intervals (Figure 13).

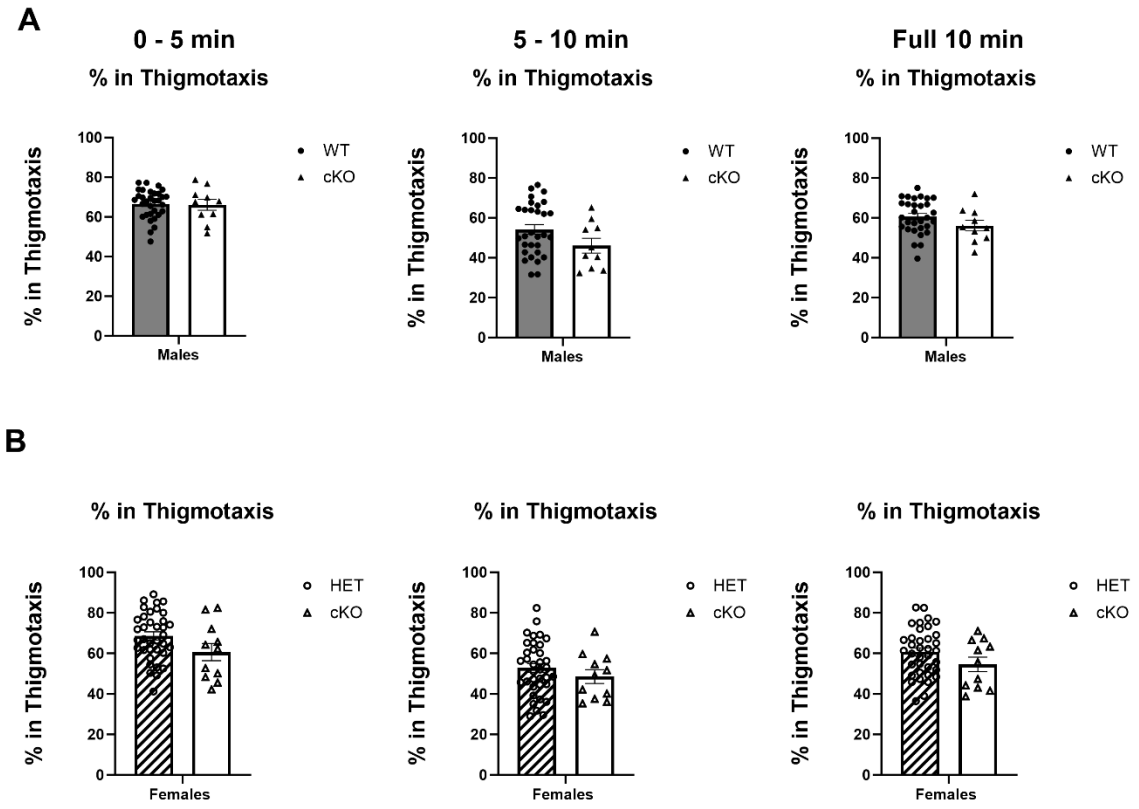

Figure 12. (A-B) Graphs describe anxiety-like behaviors observed in Thigmotaxis in the Open Field Test (OFT). A. Percent time spent in Thigmotaxis in Males. Observed no differences between WT and cKO group in the 0 – 5 min, 5 – 10 min, or the full 10 min intervals. B. Percent time spent in Open Field in Females. Observed no differences within the 0 – 5 min, 5 – 10 min, or the full 10 min intervals (WT n = 29, HET n = 34, Male cKO n = 9, Female cKO n = 11; *P < 0.05; **P < 0.01; t-test).

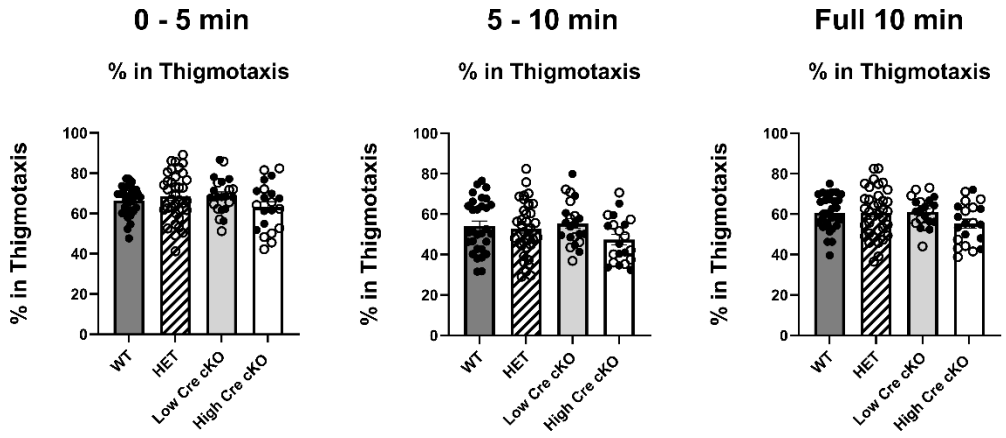

Figure 13. Graphs describe anxiety-like behaviors observed in Thigmotaxis in the Open Field Test (OFT). Observed no differences between groups within the 0 – 5 min, 5 – 10 min, or the full 10 min intervals. Indicates no significant differences in anxiety-like behaviors between the different genotypes (WT n = 29, HET n = 34, Male High Cre cKO n = 9, Female High Cre cKO n = 11; Male Low Cre cKO n = 9, Female Low Cre cKO n = 9; One-Way ANOVA followed by Tukey multiple-comparison post-test).

Elevated Plus Maze

Measurements of anxiety-like behaviors were evaluated in the Elevated Plus Maze test (EPM). One variable considered is % Time Spent in the Closed Arms. To evaluate potential sex differences, the cKO was compared to the WT and HET groups in the males and females. In the Male Group, no differences were observed in the 0 – 5 min, 5 – 10 min, or the full 10 min intervals (Figure 14A). In the Female Group, no differences were observed in the 0 – 5 min, 5 – 10 min, or the full 10 min intervals (Figure 14B). Differences were also assessed across the different genotypes. There were no observed differences were observed in the 0 – 5 min, 5 – 10 min, or the full 10 min intervals (Figure 15).

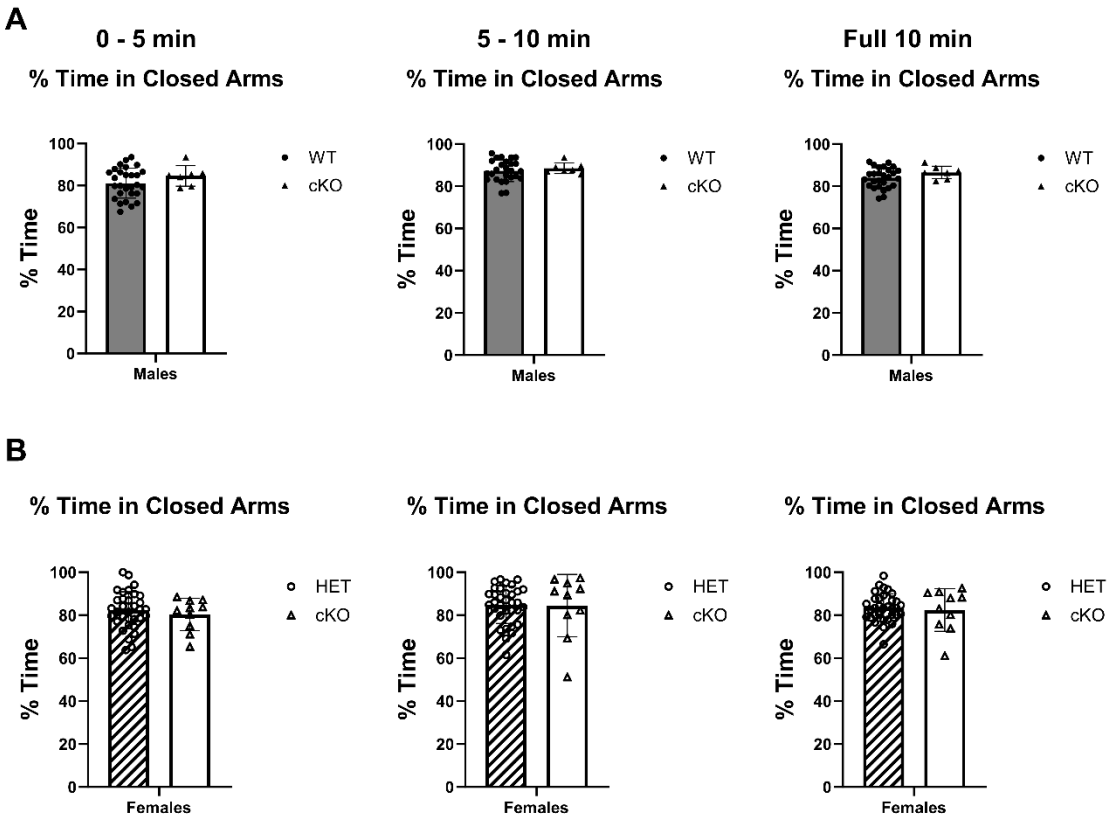

Figure 14. (A-B) Graphs describe anxiety-like behaviors observed in Closed Arms in the Elevated Plus Maze Test (EPM). A. % Time in Closed Arms in Males. Observed no differences between groups within the 0 – 5 min, 5 – 10 min, or the full 10 min intervals. Indicates no significant differences in anxiety-like behaviors between the WT and cKO. B. % Time in the Closed Arms in Females. Observed no differences between groups within the 0 – 5 min, 5 – 10 min, or the full 10 min intervals. Indicates no significant differences in anxiety-like behaviors between the WT and cKO (WT n = 29, HET n = 34, Male cKO n = 9, Female cKO n = 10; t-test).

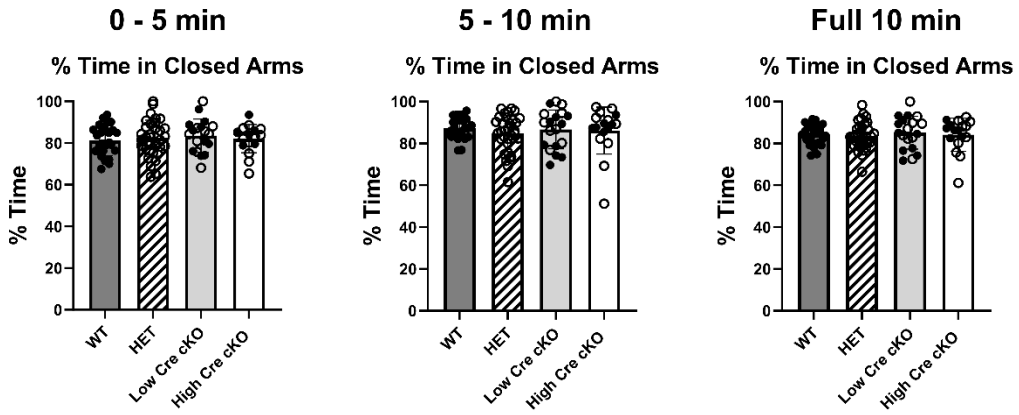

Figure 15. Graphs describe anxiety-like behaviors observed in the Closed Arms in the Elevated Plus Maze Test (EPM). Observed no differences between groups within the 0 – 5 min, 5 – 10 min, or the full 10 min intervals. Indicates no significant differences in anxiety-like behaviors between the different genotypes (WT n = 29, HET n = 34, Male High Cre cKO n = 9, Female High Cre cKO n = 10, Male Low Cre cKO n = 9, Female Low Cre cKO n = 9; One-Way ANOVA followed by Tukey multiple-comparison post-test).

Measurements of anxiety-like behaviors were evaluated in the Elevated Plus Maze test (EPM). One variable considered is % Time Spent in the Open Arms. To evaluate potential sex differences, the cKO was compared to the WT and HET groups in the males and females. In the Male Group, no differences were observed in the 0 – 5 min, 5 – 10 min, or the full 10 min intervals (Figure 16A). In the Female Group, no differences were observed in the 0 – 5 min, 5 – 10 min, or the full 10 min intervals (Figure 16B). Differences were also assessed across the different genotypes. There were no observed differences were observed in the 0 – 5 min, 5 – 10 min, or the full 10 min intervals (Figure 17).

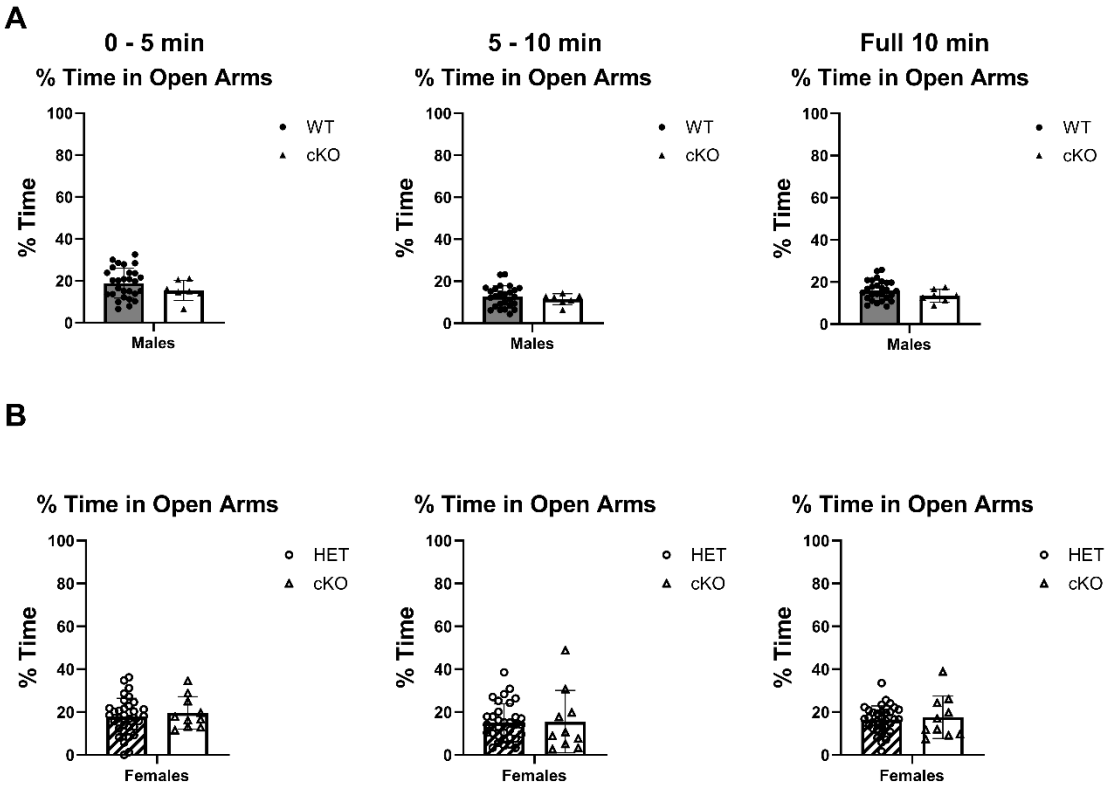

Figure 16. (A-B) Graphs describe anxiety-like behaviors observed in the Open Arms in the Elevated Plus Maze Test (EPM). A. % Time in Open Arms in Males. Observed no differences between groups within the 0 – 5 min, 5 – 10 min, or the full 10 min intervals. Indicates no significant differences in anxiety-like behaviors between the WT and cKO. B. % Time in the Open Arms in Females. Observed no differences between groups within the 0 – 5 min, 5 – 10 min, or the full 10 min intervals. Indicates no significant differences in hyperactivity between the WT and cKO (WT n = 29, HET n = 34, Male cKO n = 9, Female cKO n = 10; t-test).

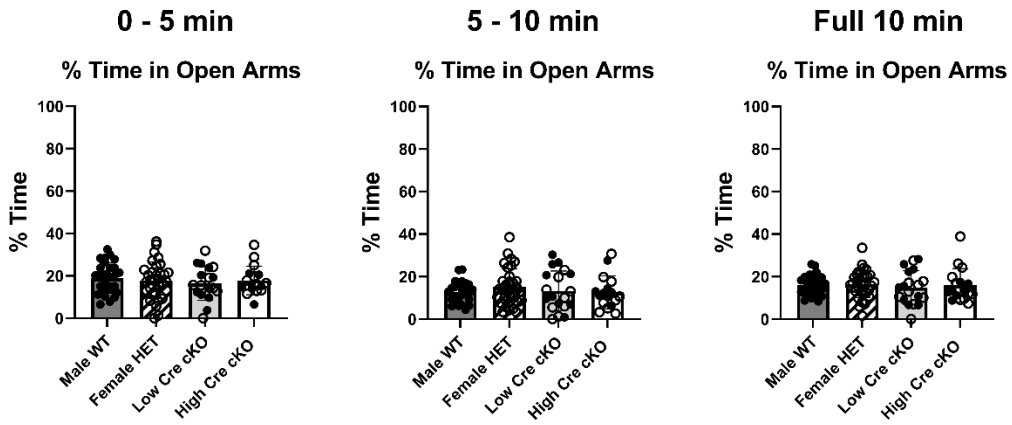

Figure 17. Graphs describe anxiety-like behaviors observed in the Open Arms in the Elevated Plus Maze Test (EPM). Observed no differences between groups within the 0 – 5 min, 5 – 10 min, or the full 10 min intervals. Indicates no significant differences in anxiety-like behaviors between the different genotypes (WT n = 29, HET n = 34, Male High Cre cKO n = 9, Female High Cre cKO n = 10, Male Low Cre cKO n = 9, Female Low Cre cKO n = 9; One-Way ANOVA followed by Tukey multiple-comparison post-test).

Measurements of hyperactivity were evaluated in the Elevated Plus Maze test (EPM). Another variable considered is Velocity in the Whole Arena. To evaluate potential sex differences, the cKO was compared to the WT and HET groups in the males and females. In the Male Group, no differences were observed in the 0 – 5 min, 5 – 10 min, or the full 10 min intervals (Figure 18A). In the Female Group, no differences were observed in the 0 – 5 min, 5 – 10 min, or the full 10 min intervals (Figure 18B). Differences were also assessed across the different genotypes. Across genotypes, no differences were observed in the 0 – 5 min, 5 – 10 min, or the full 10 min intervals (Figure 19).

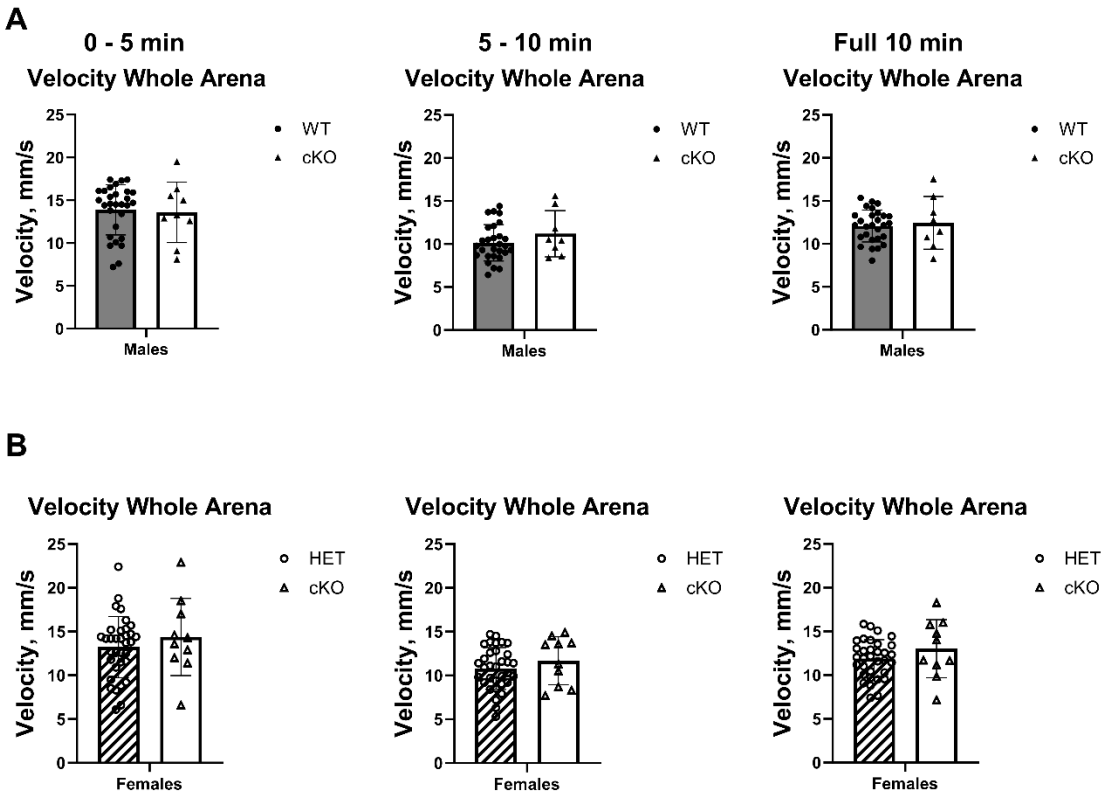

Figure 18. (A-B) Graphs describe hyperactivity observed in the Whole Arena in the Elevated Plus Maze Test (EPM). A. Velocity in the Whole Arena in Males. Observed no differences between groups within the 0 – 5 min, 5 – 10 min, or the full 10 min intervals. Indicates no significant differences in hyperactivity between the WT and cKO. B. Velocity in the Whole Arena in Females. Observed no differences between groups within the 0 – 5 min, 5 – 10 min, or the full 10 min intervals. Indicates no significant differences in hyperactivity between the HET and cKO (WT n = 29, HET n = 34, Male cKO n = 9, Female cKO n = 10; t-test).

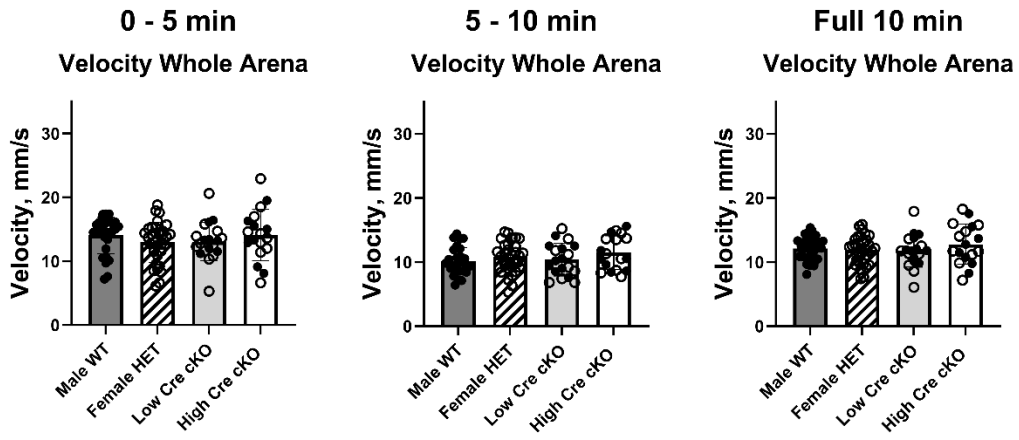

Figure 19. Graphs describe measurements of hyperactivity in the Elevated Plus Maze Test (EPM). Observed differences between the HET and High Cre cKO during the 0 – 5 min intervals. Observed no differences between groups within the 0 – 5 min, 5 – 10 min, or the full 10 min intervals. Indicates no significant differences in hyperactivity between the different genotypes (WT n = 29, HET n = 34, Male High Cre cKO n = 9, Female High Cre cKO n = 10, Male Low Cre cKO n = 9, Female Low Cre cKO n = 9; One-Way ANOVA followed by Tukey multiple-comparison post-test).

Measurements of hyperactivity were evaluated in the Elevated Plus Maze test (EPM). Another variable considered is Velocity in the Open Arms. To evaluate potential sex differences, the cKO was compared to the WT and HET groups in the males and females. In the Male Group, no differences were observed in the 0 – 5 min, 5 – 10 min, or the full 10 min intervals (Figure 20A). In the Female Group, no differences were observed in the 0 – 5 min, 5 – 10 min, or the full 10 min intervals (Figure 20B). Differences were also assessed across the different genotypes. Across genotypes, no differences were observed in the 0 – 5 min, 5 – 10 min, or the full 10 min intervals (Figure 21).

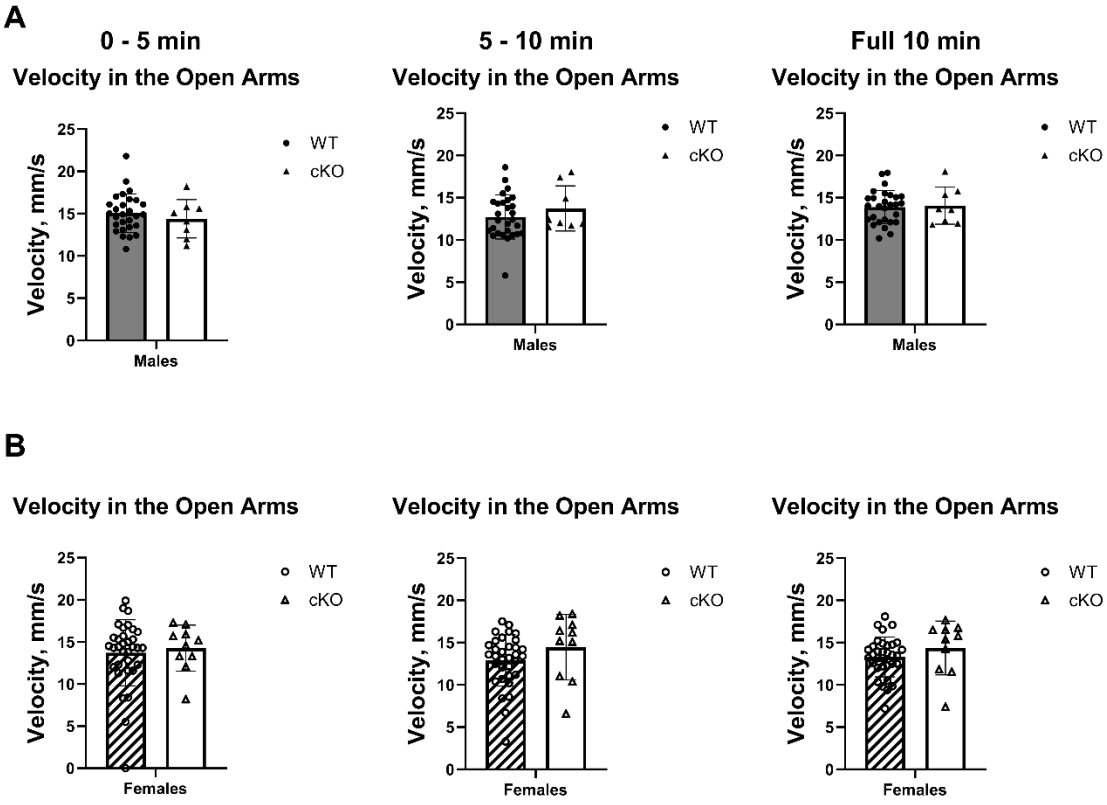

Figure 20. (A-B) Graphs describe hyperactivity observed in the Open Arms in the Elevated Plus Maze Test (EPM). A. Velocity in the Open Arms in Males. Observed no differences between groups within the 0 – 5 min, 5 – 10 min, or the full 10 min intervals. Indicates no significant differences in hyperactivity between the WT and cKO. B. Velocity in the Open Arms in Females. Observed no differences between groups within the 0 – 5 min, 5 – 10 min, or the full 10 min intervals. Indicates no significant differences in hyperactivity between the HET and cKO (WT n = 29, HET n = 34, Male cKO n = 9, Female cKO n = 10; t-test).

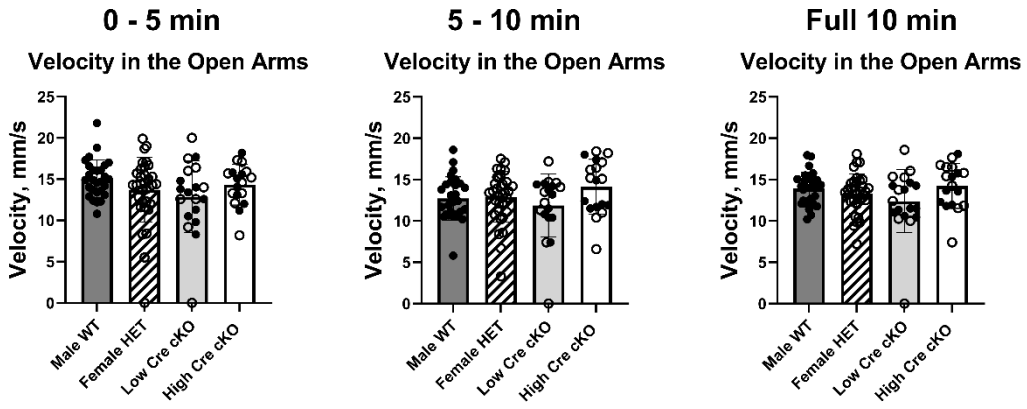

Figure 21. Graphs describe measurements of hyperactivity in the Open Arms in the Elevated Plus Maze Test (EPM). Observed differences between the HET and High Cre cKO during the 0 – 5 min intervals. Observed no differences between groups within the 0 – 5 min, 5 – 10 min, or the full 10 min intervals. Indicates no significant differences in hyperactivity between the different genotypes (WT n = 29, HET n = 34, Male High Cre cKO n = 9, Female High Cre cKO n = 10, Male Low Cre cKO n = 9, Female Low Cre cKO n = 9; One-Way ANOVA followed by Tukey multiple-comparison post-test).

Measurements of hyperactivity were evaluated in the Elevated Plus Maze test (EPM). Another variable considered is Velocity in the Closed Arms. To evaluate potential sex differences, the cKO was compared to the WT and HET groups in the males and females. In the Male Group, no differences were observed in the 0 – 5 min, 5 – 10 min, or the full 10 min intervals (Figure 22A). In the Female Group, no differences were observed in the 0 – 5 min, 5 – 10 min, or the full 10 min intervals (Figure 22B). Differences were also assessed across the different genotypes. Across genotypes, no differences were observed in the 0 – 5 min, 5 – 10 min, or the full 10 min intervals (Figure 23).

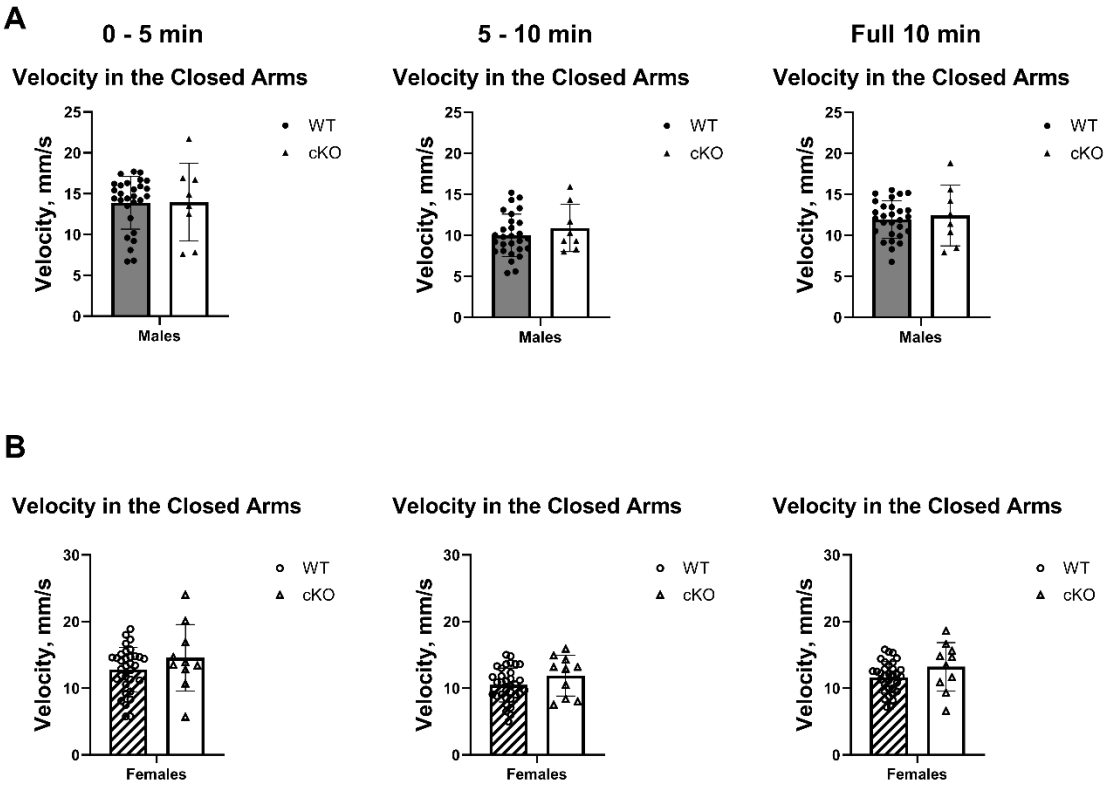

Figure 22. (A-B) Graphs describe hyperactivity observed in the Closed Arms in the Elevated Plus Maze Test (EPM). A. Velocity in the Closed Arms in Males. Observed no differences between groups within the 0 – 5 min, 5 – 10 min, or the full 10 min intervals. Indicates no significant differences in hyperactivity between the WT and cKO. B. Velocity in the Closed Arms in Females. Observed no differences between groups within the 0 – 5 min, 5 – 10 min, or the full 10 min intervals. Indicates no significant differences in hyperactivity between the HET and cKO (WT n = 29, HET n = 34, Male cKO n = 9, Female cKO n = 10; t-test).

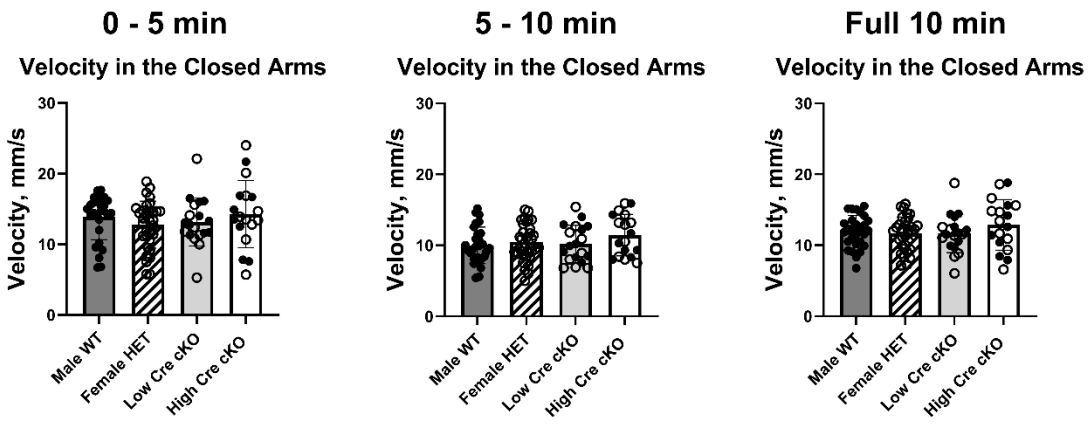

Figure 23. Graphs describe measurements of hyperactivity in the Closed Arms in the Elevated Plus Maze Test (EPM). Observed no differences between groups within the 0 – 5 min, 5 – 10 min, or the full 10 min intervals. Indicates no significant differences in hyperactivity between the different genotypes (WT n = 29, HET n = 34, Male High Cre cKO n = 9, Female High Cre cKO n = 10, Male Low Cre cKO n = 9, Female Low Cre cKO n = 9; One-Way ANOVA followed by Tukey multiple-comparison post-test).

Social Novelty Test

Measurements of Sociability were evaluated in the Social Novelty Test (SNT). In the first part of the Social Novelty Test, Sociability Index is calculated. To evaluate potential sex differences, the cKO was compared to the WT and HET groups in the males and females. In the Male Group, no differences were observed in the 0 – 5 min, 5 – 10 min, or the full 10 min intervals (Figure 24A). In the Female Group, no differences were observed in the 0 – 5 min, 5 – 10 min, or the full 10 min intervals (Figure 24B). Differences were also assessed across the different genotypes. Across genotypes, no differences were observed in the 0 – 5 min, 5 – 10 min, or the full 10 min intervals (Figure 25).

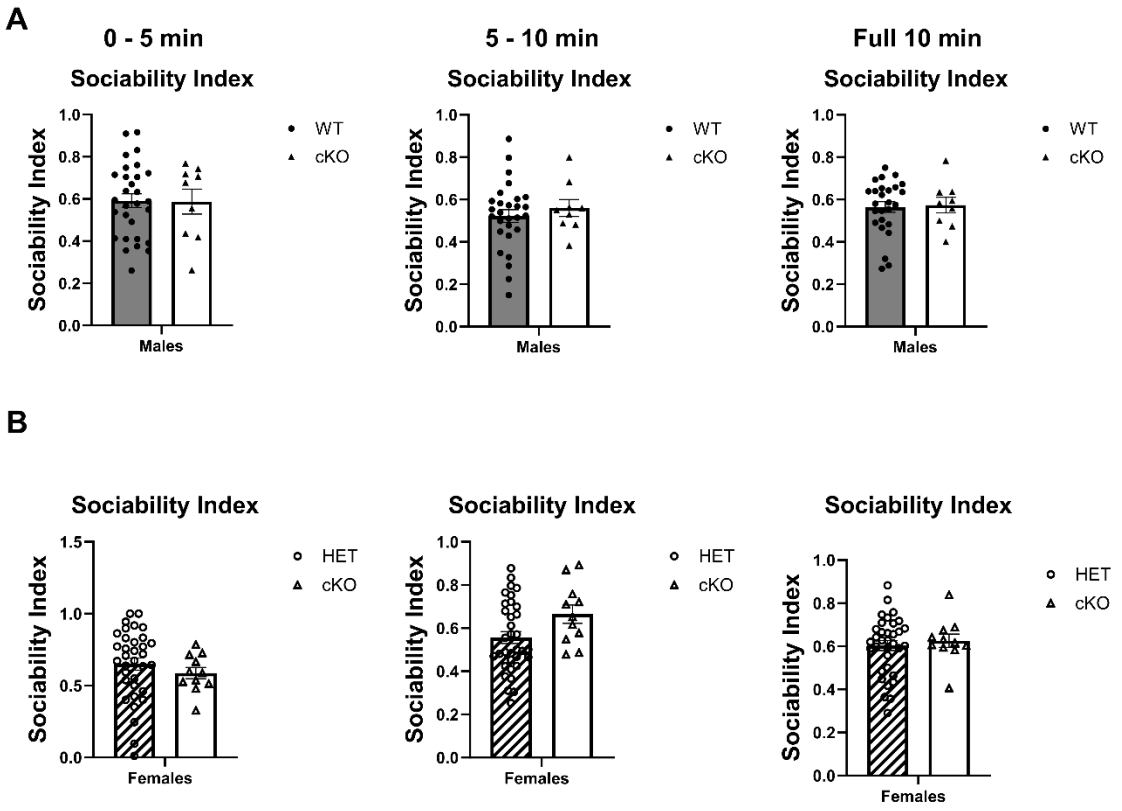

Figure 24. (A-B) Graphs describe Sociability observed in the Stranger 1 Assessment in the Social Novelty Test (SNT). A. Sociability Index for Males. Observed no differences between groups within the 0 – 5 min, 5 – 10 min, or the full 10 min intervals between the WT and cKO. This indicates no significant difference in Sociability between the WT and cKO. B. Sociability Index for Females. Observed no differences between groups within the 0 – 5 min, 5 – 10 min, or the full 10 min intervals between HET and cKO. This indicates no significant difference in Sociability between the HET and cKO (WT n = 28, HET n = 34, Male cKO n = 9, Female cKO n = 11; t-test).

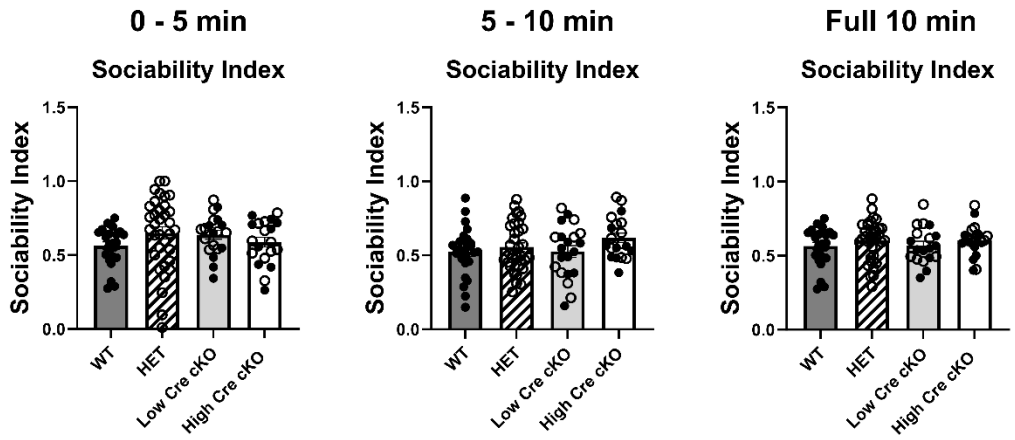

Figure 25. Graphs describe Sociability observed in the Stranger 1 Assessment in the Social Novelty Test (SNT). Observed no differences between genotype groups within the 0 – 5 min, 5 – 10 min, or the full 10 min intervals between WT, HET, Low Cre cKO, and High Cre cKO (WT n = 29, HET n = 34, Male High Cre cKO n = 9, Female High Cre cKO n = 11, Male Low Cre cKO n = 12, Female Low Cre cKO n = 9; One-Way ANOVA followed by Tukey multiple-comparison post-test).

Measurements of Social Novelty Preference were evaluated in the Social Novelty Test (SNT). In the second part of the Social Novelty Test, the Social Novelty Preference index is calculated. To evaluate potential sex differences, the cKO was compared to the WT and HET groups in the males and females. In the Male Group, no differences were observed in the 0 – 5 min, 5 – 10 min, or the full 10 min intervals (Figure 26A). In the Female Group, no differences were observed in the 0 – 5 min, 5 – 10 min, or the full 10 min intervals (Figure 26B). Differences were also assessed across the different genotypes. Across genotypes, no differences were observed in the 0 – 5 min or the full 10 min intervals. During the 5 – 10 min interval, the Low Cre cKO group showed differences compared to the WT group with the Low Cre cKO group showing a higher preference for the novel mouse compared to the WT (Figure 27).

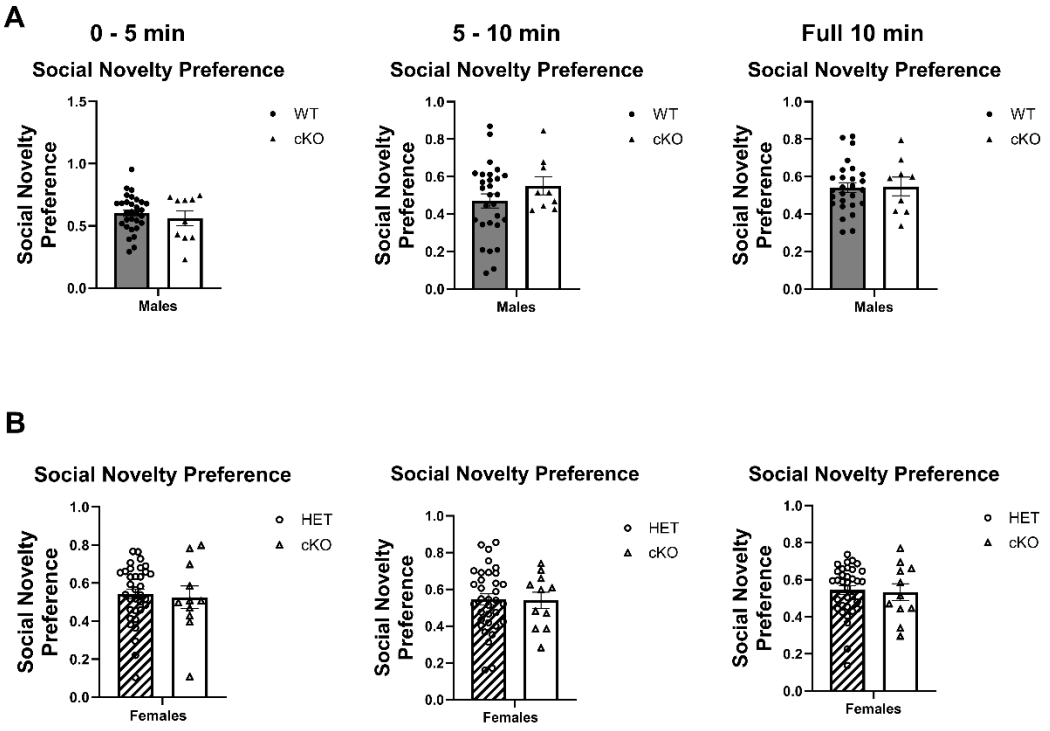

Figure 26. (A-B) Graphs describe Social Novelty Preference observed in the Stranger 2 Assessment in the Social Novelty Test (SNT). A. Social Novelty Preference for Males. Observed no differences between groups within the 0 – 5 min, 5 – 10 min, or the full 10 min intervals between WT and cKO. B. Social Novelty Preference for Females. Observed no differences between groups within the 0 – 5 min, 5 – 10 min, or the full 10 min intervals between HET and cKO (WT n = 28, HET n = 34, Male cKO n = 9, Female cKO n = 11; t-test).

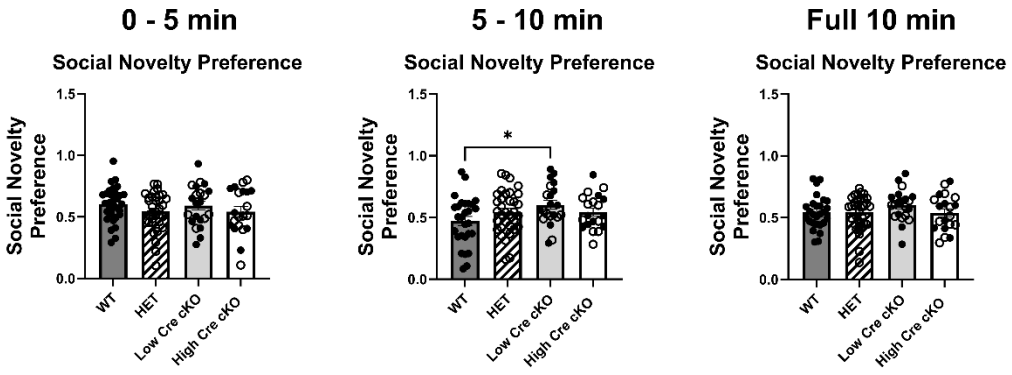

Figure 27. Graphs describe Social Novelty Preference observed in the Stranger 2 Assessment in the Social Novelty Test (SNT). Observed no differences between genotype groups within the 0 – 5 min or full 10 min intervals between WT, HET, Low Cre cKO, and High Cre cKO. Observed differences between the Low Cre KO and WT in the 5 – 10 min interval (WT n = 29, HET n = 34, Male High Cre cKO n = 9, Female High Cre cKO n = 11, Male Low Cre cKO n = 12, Female Low Cre cKO n = 9; *P < 0.05; One-Way ANOVA followed by Tukey multiple-comparison post-test).

In the Social Novelty Test (SNT), we evaluated the Percent Time Spent with Stranger in both parts of the Social Novelty Test. An index was calculated by determining the Time (Minutes) Spent with Stranger 1 in the Sociability Assessment in the 1st 5 Minutes compared to the total time spent with Stranger 1 and converting this number to a percent. The same index was also calculated to determine the % Time Spent with Stranger 2 in the Social Novelty Preference Assessment. Differences were also assessed across the different genotypes. Across genotypes, no differences in % Time Spent with Stranger 1 were observed between the WT, HET, Low Cre cKO, and High Cre cKO (Figure 28A). Across genotypes, differences in % Time Spent with Stranger 2 were observed between the WT when compared to the HET, Low Cre cKO, and High Cre cKO groups. The WT spent a greater percentage of time with Stranger 2 during the 0 – 5 min interval of the test, then lost preference for the novel mouse. However, the HET, Low Cre cKO, and the High Cre cKO groups did not show an interest in Stranger 2 during any of the time intervals (Figure 28B).

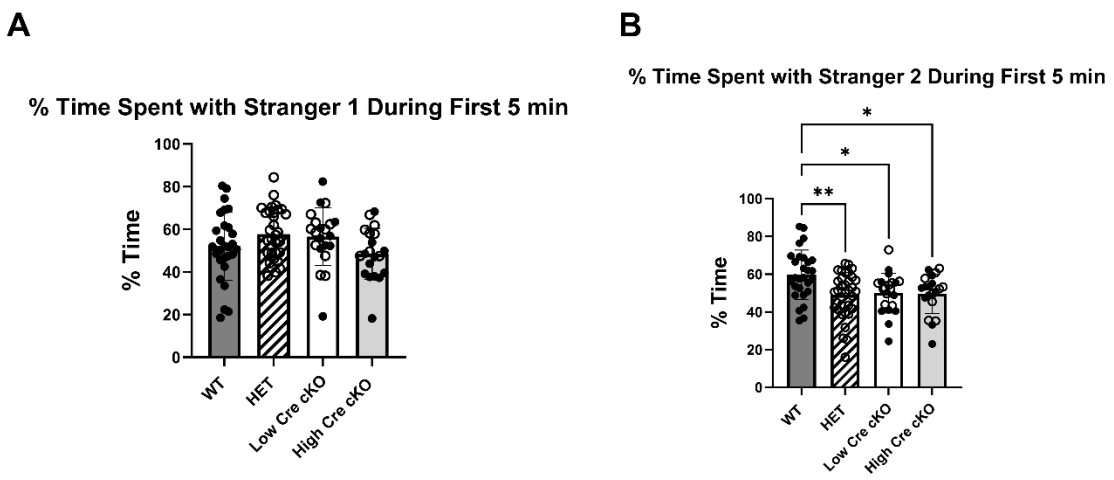

Figure 28. (A-B) Graphs describe the Percent Time Spent with Stranger 1 and 2 During the First 5 Minutes of the Social Novelty Test (SNT). A. % Time Spent with Stranger 1 During First 5 Minutes. Observed no differences in time spent with Stranger 1 between the WT, HET, Low Cre cKO, and High Cre cKO in the 0 – 5 min interval. B. % Time Spent with Stranger 2 During First 5 Minutes. Observed differences in % time spent with stranger 2 between the WT and HET, the WT and Low Cre cKO, and the WT and High Cre cKO in the 0 – 5 min interval. The WT group spends a larger percentage of time with Stranger 1 in the 0 – 5 min interval of the test compared to the HET, Low Cre cKO, and the High Cre cKO (WT n = 29, HET n = 34, Male High Cre cKO n = 9, Female High Cre cKO n = 11, Male Low Cre cKO n = 12, Female Low Cre cKO n = 9; *P < 0.05; **P < 0.01; One-Way ANOVA followed by Tukey multiple-comparison post-test).

Confocal Microscopy

A representative image was taken of the Hippocampus in a P28 mouse. A co-stain for FMRP, Glutamine Synthetase (GS), and DAPI was performed. This confocal image consists of a z-stack 10 µm thick with image increments of 2 µm. The white arrow points toward FMRP-stained cells, and the orange arrow points toward GS-stained astrocytes. In this representative image, the cell-specific knock-out is confirmed by the lack of overlap between the FMRP stain and the astrocytic stain.

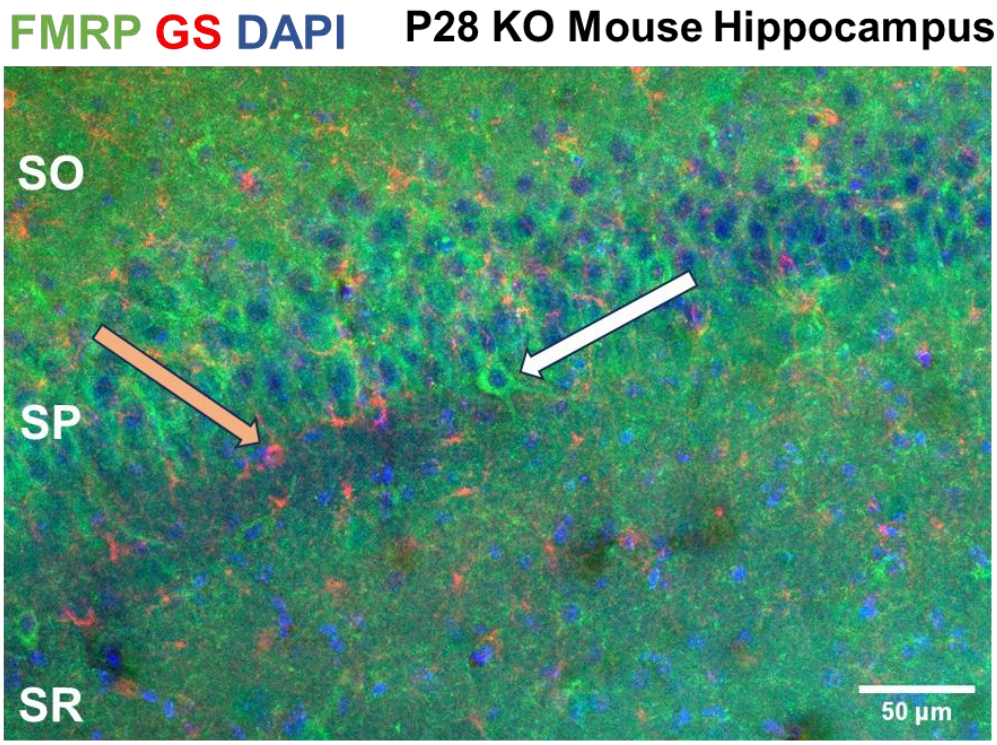

Figure 29. Representative Confocal Images showing FMRP (green), GS (red), and DAPI (blue) in the hippocampus of a P28 Astrocyte-Specific KO Mouse. Confocal images were taken to form a Z-stack with 20X objectives.

Tiled images were taken of frontal and middle coronal slices collected from P28 WT and cKO mice expressing the red fluorescent protein reporter tdTomato. The tiled image consists of a z-stack 80 µm thick with image increments of 10 µm. These images were acquired with 5X objectives. In these tiled images, the fluorescent reporter labels astrocytes. The fluorescence from tdTomato verifies the inducible genetic recombination model.

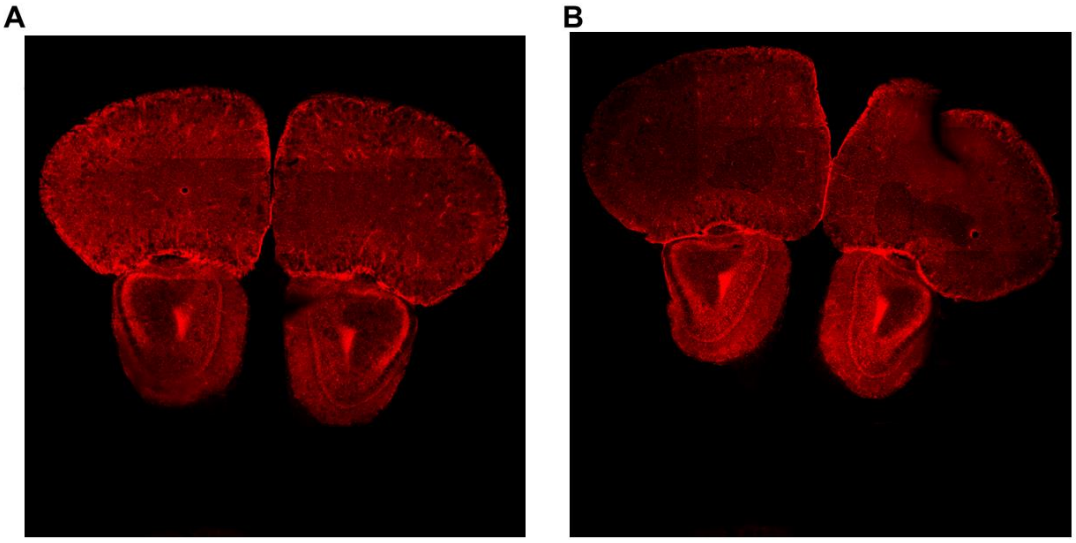

Figure 30. Tiled images of a Frontal Coronal Slice from a P28 mouse containing frontal cortex. Confocal images were taken to form a Z-stack with 5X objectives. A. Confocal image of a P28 cKO mouse expressing fluorescent reporter tdTomato in frontal astrocytes. B. Confocal image of a P28 WT mouse expressing fluorescent reporter tdTomato in frontal astrocytes.

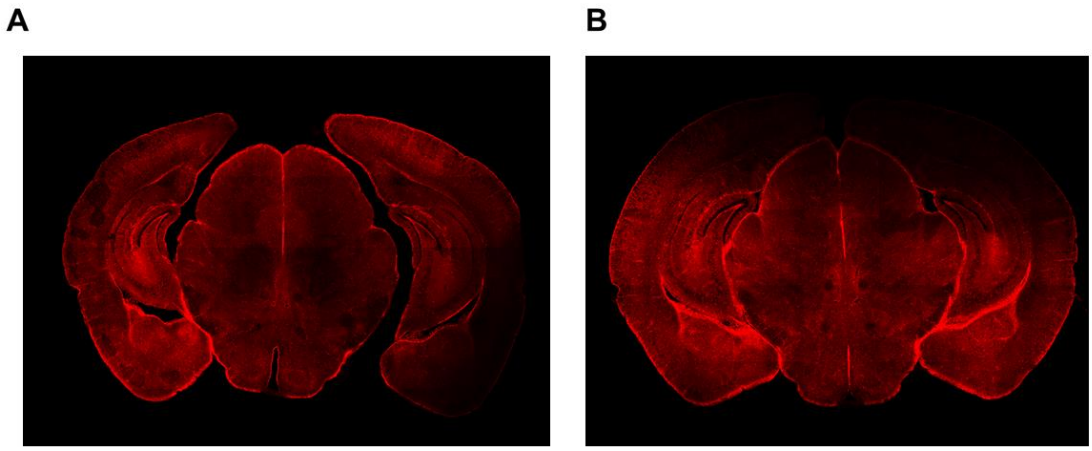

Figure 31. Tiled images of Middle Coronal Slices of a P28 Mice containing hippocampus. Confocal images were taken to form a Z-stack with 5X objectives. A. Confocal image of a P28 WT mouse expressing fluorescent reporter tdTomato in mid-brain astrocytes. B. Confocal image of a P28 cKO mouse expressing fluorescent reporter tdTomato in mid-brain astrocytes.

Confocal images were taken of frontal cortex. Frontal coronal slices were collected from P28 WT and cKO mice expressing the red fluorescent protein reporter tdTomato. The high magnification images consisted of a compressed z-stack of 2 μm intervals with a stack thickness of 10 μm. Images were acquired with 20X magnification objectives. In these high magnification images, the fluorescent reporter labels astrocytes and nuclear DNA was stained with 4′,6-diamidino-2-phenylindole (DAPI). The fluorescence from tdTomato verifies the inducible genetic recombination model.

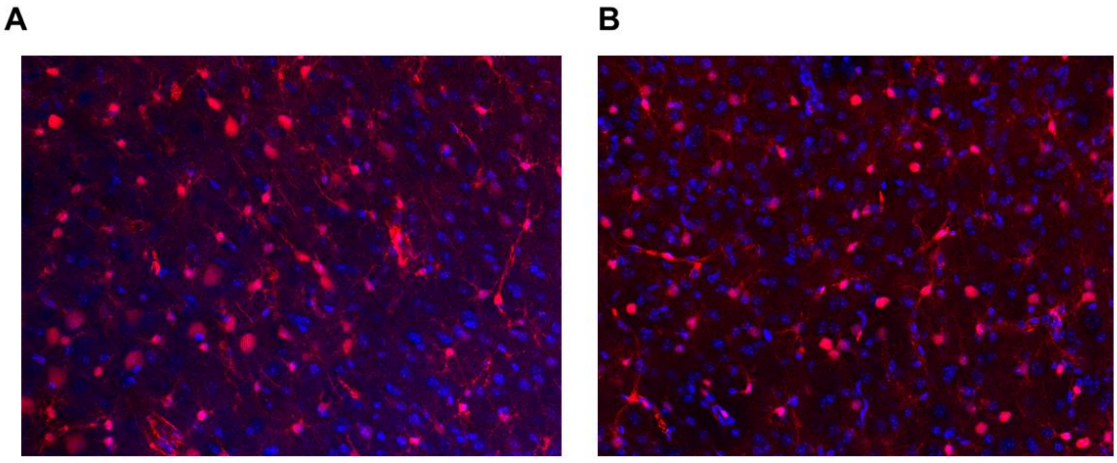

Figure 32. High Magnification images of Frontal Cortex of P28 Mice. Confocal images were taken to form a Z-stack with 20X objectives. Imaged tdTomato (red) and DAPI (blue). A. Confocal image of a P28 WT mouse expressing fluorescent reporter tdTomato in frontal cortex astrocytes. B. Confocal image of a P28 cKO mouse expressing fluorescent reporter tdTomato in frontal cortex astrocytes.

Confocal images were taken of hippocampus. Mid-brain coronal slices were collected from P28 WT and cKO mice expressing the red fluorescent protein reporter tdTomato. The high magnification images consisted of a compressed z-stack of 2 μm intervals with a stack thickness of 10 μm. Images were acquired with 20X magnification objectives. In these high magnification images, the fluorescent reporter labels astrocytes and nuclear DNA was stained with DAPI. The fluorescence from tdTomato verifies the inducible genetic recombination model.

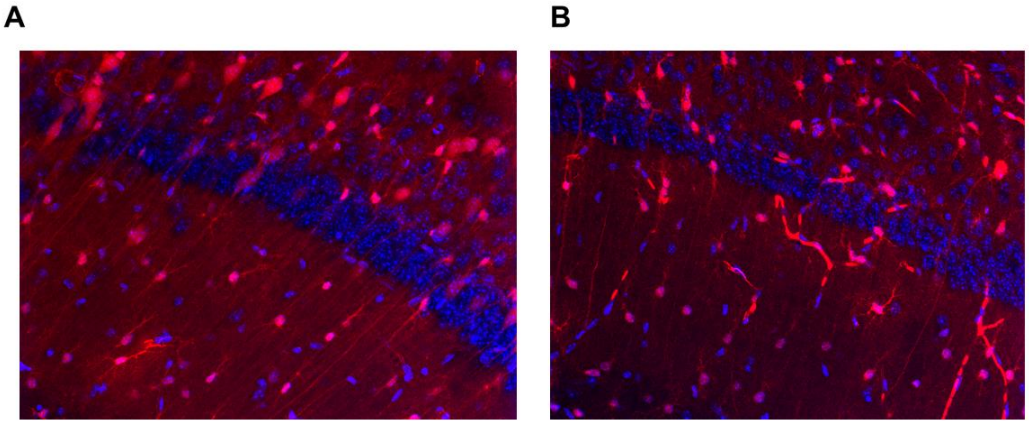

Figure 33. High Magnification images of Hippocampus of P28 Mice. Confocal images were taken to form a Z-stack with 20X objectives. Imaged tdTomato (red) and DAPI (blue). A. Confocal image of a P28 WT mouse expressing fluorescent reporter tdTomato in hippocampal astrocytes. B. Confocal image of a P28 cKO mouse expressing fluorescent reporter tdTomato in hippocampal astrocytes.

Confocal images were taken of auditory cortex. Mid-brain coronal slices were collected from P28 WT and cKO mice expressing the red fluorescent protein reporter tdTomato. The high magnification images consisted of a compressed z-stack of 2 μm intervals with a stack thickness of 10 μm. Images were acquired with 20X magnification objectives. In these high magnification images, the fluorescent reporter labels astrocytes and nuclear DNA was stained with DAPI. The fluorescence from tdTomato verifies the inducible genetic recombination model.

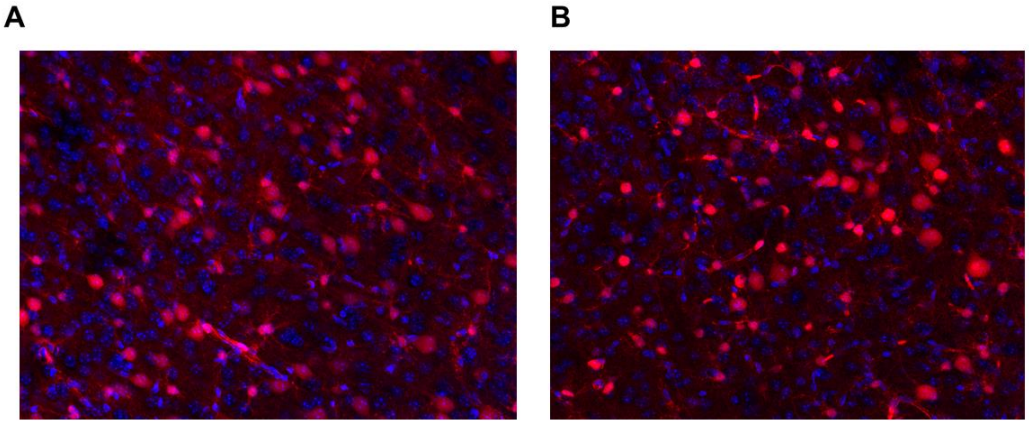

Figure 34. High Magnification images of Auditory Cortex of P28 Mice. Confocal images were taken to form a Z-stack with 20X objectives. Imaged tdTomato (red) and DAPI (blue). A. Confocal image of a P28 WT mouse expressing fluorescent reporter tdTomato in auditory cortex astrocytes. B. Confocal image of a P28 cKO mouse expressing fluorescent reporter tdTomato in auditory cortex astrocytes.

DISCUSSION

Previous observations in mouse models of Fragile X Syndrome have demonstrated the influence of the *FMR1* deletion and absence of FMRP on behavior abnormalities. Furthermore, increasing research is demonstrating the importance of astrocytes in modulating synaptic connections in development. Dysfunction of these glial cells contributes to behavioral deficits associated with Fragile X Syndrome. This thesis project delineates the role of developmental astrocyte-specific deletions of FMRP and its consequences on altering behavior. The primary findings support that a developmental astrocyte-specific deletion of *FMR1* induces similar behavioral abnormalities in the cKO as observed in the global KO. The deletion of the *FMR1* gene from astrocytes during a developmental time point crucial for inhibitory circuit development contributes to increased locomotive activity without showing differences in anxiety-like behaviors. Furthermore, the HET observed in this model is an intermediate phenotype that behaves similarly to the WT in the context of hyperactivity and similarly to the cKO during social memory tasks.

Behavioral Differences Observed in the Conditional Knock-Out

First, our findings demonstrate increased hyperactivity and distance traveled by the cKO mice during the Open Field Test. However, these observations are absent in the Elevated Plus Maze test. The increase in locomotor activity could be explained by astrocytic involvement in modulating behavior. Astrocytes play a role in cognition, motor activity, emotion, and sensory processing (Oliveira, 2015). Our results suggest that the timing of

FMR1 deletion from astrocytes may differentially affect neuronal activity in different brain areas which could explain differences in behavioral phenotypes.

Secondly, our findings also suggest that contextual factors play a role in locomotion. Although the hyperactive behavior manifested during the Open Field Test, this was not observed in the following Elevated Plus Maze test. In the Elevated Plus Maze, our data demonstrates that there are no differences in locomotor activity between the WT, HET, Low Cre cKO, and High Cre cKO. This suggests that in this assessment, there is no significant difference in hyperactivity in the cKO compared to the WT and HET. However, consistent with our findings in the Open Field Test, there are no differences in anxiety-like behaviors between the WT and HET when compared to the cKO. This suggests that the cKO does not display anxiety-like behaviors like the Global KO.

Our findings also indicate that there is abnormal socialization in the cKO compared to the WT and HET groups. This abnormality is time-dependent, with WT mice initially having preference towards a novel mouse compared to a familiar mouse then losing preference. In contrast, the KO mouse lacks preference towards the novel mouse at any of the time points during the test. This could be the result of habituation or impaired social memory or preference for the KO group.

The hippocampus is an important area for social memory processing, and disruption of the hippocampus contributes to impairments in social recognition (Maaswinkel, 1996). The promoter used for the transgenic mice in this study was the GFAP promoter, so astrocytes expressing GFAP would express the genetic manipulation. There is a high

concentration of GFAP-positive astrocytes in the hippocamps, making it an effective astrocytic marker (Zhang, 2019). The differences we observe in the cKO could potentially be explained by the greater expression of GFAP in the hippocampus. Using a mouse model where genetic recombination is driven by the GFAP promoter, there could be greater genetic recombination occurring during the developmental deletion; thus, affecting behavior associated with this brain area. This could potentially explain the differences we observe in the Social Novelty Test where the Heterozygous, Low Cre cKO, and High Cre cKO lack interest in the novel mouse during the first 5 minutes of the assessment unlike the Wild-Type.

Heterozygous Astrocyte-Specific Model Behavioral Alterations

Our findings indicate that the behaviors of the heterozygous model are also dependent on the behavioral context. In the Open Field Test, the Heterozygous group was found to have similarities to the Wild-Type male group. In both the whole arena and in thigmotaxis, the heterozygous females traveled less distance compared to the Conditional Knock-Out females. In the One-Way ANOVA analysis, the Heterozygous females were found to have no significant differences when compared to the male Wild-Type mice. However, differences were observed between the Heterozygous group and both the male and female Conditional Knock-Out groups. The Conditional Knock-Out mice traveled more distance and moved at a higher velocity compared to the Heterozygous females.

One other notable difference observed in the Heterozygous group is the similarities to the Conditional Knock-Out group during the Social Novelty Test. During the first 5 minutes

of the Social Novelty Test, the Wild-Type mice spent more time with Stranger 2. After the first 5 minutes, the Wild-Type mice would no longer show this preference. However, the Heterozygous females behaved similarly to both the Conditional Knock-Out males and females, and the Heterozygous mice did not show preference towards Stranger 2 at any of the time points. The observed differences between the Wild-Type and the Heterozygous suggests that the Heterozygous mice behave similarly to the Conditional Knock-Out mice while showing abnormal social preference.

Together, these findings suggest that the Heterozygous mice are an intermediate group that demonstrates similarities to both the Wild-Type or the Conditional Knock-Out groups depending on the behavioral assessment. However, limited data exists for the heterozygous mouse models and there are fewer studies conducted on heterozygous mice under the conditional astrocyte-specific KO when compared to the male Global WT/KO models.

Global FMR1 KO Behavioral Phenotypes

However, despite Fragile X Syndrome-like behavioral abnormalities observed in the model, previous findings have remained inconsistent. Previous studies evaluating behavioral phenotypes in the global knock-out show varying results. One study using the Elevated Plus Maze test (EPM) found P21 *FMR1* KO mice spent significantly less time in the open arms compared to WT, demonstrating increased anxiety (Bilousova, 2008). Another study using *FMR1* KO mice aged 3 months found similar results with increased hyperactive behavior and time spent in the closed arms (Yuskaitis, 2010). However,

another study using P66 mice found that there were no genotype differences in the locomotion and time spent in the closed arms between the *FMR1* KO and WT in the EPM (Mineur, 2002). There were also no genotype differences observed in the amount of time spent in the closed arms versus open arms between the *FMR1* KO and WT in mice tested at 12-15 weeks (Nielsen, 2002).

In an Open Field Test (OFT) assessment of behavior, one study found that *FMR1* KO mice aged 3-4 months showed increased locomotion compared to the WT, and the *FMR1* KO spent more time in the open field compared to the WT (Peier, 2000). Previous work done with *FMR1* KO mice aged 3 months showed increased locomotion along with increased time spent in the open field compared to the WT (Yuskaitis, 2010). In mice aged 8 weeks, an OFT assessment found that *FMR1* KO mice spent less time in thigmotaxis compared to the WT, but the number of entries into the open field was not statistically significant between the two genotypes (Liu, 2011). In animals tested once a day for five consecutive days between 3-5 weeks of age, one study found there were consistent genotype differences where the *FMR1* KO would spend more time in the open field compared to the WT mice (Yan, 2004).

In the Social Novelty Test (SNT), results were also variable in the global *FMR1* KO condition. In one study evaluating mice through the SNT, the results indicated that there was no significant preference toward the novel mouse in the *FMR1* KO compared to the WT mice (Dahlhaus, 2010). Similarly, another study investigating 10–12-month age *FMR1* KO mice found that the *FMR1* KO mice demonstrated less sniffing behavior

toward the novel mouse when compared to the WT, suggesting anxiety-like behavior (McNaughton, 2008).

CONCLUSION

I am reporting a study that demonstrates how the behavioral phenotype of a developmental astrocyte-specific deletion of *FMR1* compared to the WT and HET condition. The data shows there are no substantial sex differences observed between the males and females during the behavioral assessments. However, there are significant genotype differences observed during testing. Overall, the cKO shows increased hyperactivity compared to the WT and HET condition across both sexes. The results from the Open Field Test demonstrate that the astrocyte-specific knock-out model of Fragile X Syndrome mice do not demonstrate differences in anxiety-related behaviors but show increase locomotion. The increase in cKO locomotion in the open field and thigmotaxis is indicative of hyperactive behavior observed as a Fragile X Syndrome-like phenotype. In the Elevated Plus Maze test, we do not see any difference between genotypes in the amount of time spent in the open arms versus the closed arms. Therefore, there are no observed genotype differences in anxiety-like behaviors. In the Elevated Plus Maze test, we also do not see a significant change in locomotive activity based on the number of bouts or velocity in the arena. In the Social Novelty Test, we noticed there are no differences between genotypes in the 1st 5 minutes, 2nd 5 minutes, or the full 10-minute experimental duration. However, we found that WT mice exhibit more interest in the novel mouse in the 1st 5 minutes while cKO mice do not show preference between the 1st and 2nd 5-minute intervals, demonstrating there are time-dependent social abnormalities in the cKO versus the WT. While differences we observed between the WT and cKO and

the HET and cKO, we noticed that HET females behaved similarly to the male WT mice, so no significant differences were found between the two groups.

Together, these behavioral assessment findings are different from previously reported work in the global KO model. Our findings also demonstrate that Cre expression of the cKO is a factor to consider when comparing differences between the WT and cKO groups. The data indicated the cKO mice with high Cre expression behaved similarly to global KO mice, while cKO mice with low Cre expression behaved similarly to the WT and HET mice. These findings also suggest that the developmental timing of the astrocyte *FMR1* deletion would affect neuronal activity in different brain areas, leading to different behavioral outcomes. Future studies may investigate differential timing of astrocytic *FMR1* deletion and assess the resulting impact on behavioral outcomes.

Future work can further expand on this project by utilizing immunohistochemistry to co-stain for astrocytes and both astrocytic and neuronal FMRP. This future work will provide insight into the brain areas most affected by the *FMR1* deletion during this developmental timepoint and lay the foundation for targeted gene reactivation therapy. Additionally, another symptom of Fragile X Syndrome is susceptibility to seizures. The current mouse strain our model uses, C57BL/6J, is found to be resistant to audiogenic seizures (Copping, 2019). By using a different mouse strain for the model or by modifying the age of seizure testing, future studies can study the impact of astrocytic *FMR1* deletion on seizure susceptibility and intensity.

Currently, there is limited data available on Heterozygous mice in the astrocyte-specific *FMR1* deletion model. Our findings show that the Heterozygous demonstrate intermediate behavioral phenotypes, and their behavior can resemble the Wild-Type or Conditional Knock-Out mice depending on the assessment performed. Future work can expand on these findings by performing other behavioral assessments to further compare the Wild-Type, Conditional Knock-Out, and Heterozygous mice and characterize their behavioral phenotypes. Other autism-like behaviors can be evaluated with behavior tests such as Morris Water Maze, Probabilistic Reversal Learning Test, or evaluating other anxiety-like behaviors such as grooming or rearing to determine further differences or similarities between the Heterozygous group and the Wild-Type and Conditional Knock-Out groups.

REFERENCES

1. Bilousova, T. V., Dansie, L., Ngo, M., Aye, J., Charles, J. R., Ethell, D. W., & Ethell, I. M. (2008). Minocycline promotes dendritic spine maturation and improves behavioural performance in the Fragile X Mouse Model. *Journal of Medical Genetics*, *46*(2), 94–102. https://doi.org/10.1136/jmg.2008.061796

2. Boggs, A. E., Schmitt, L. M., McLane, R. D., Adayev, T., LaFauci, G., Horn, P. S., Dominick, K. C., Gross, C., & Erickson, C. A. (2022). Optimization, validation and initial clinical implications of a LUMINEX-based immunoassay for the quantification of fragile x protein from dried blood spots. *Scientific Reports*, *12*(1). https://doi.org/10.1038/s41598-022-09633-8

3. Bostrom, C., Yau, S., Majaess, N., Vetrici, M., Gil-Mohapel, J., & Christie, B. R. (2016). Hippocampal dysfunction and cognitive impairment in fragile-X syndrome. *Neuroscience & Biobehavioral Reviews*, *68*, 563–574. https://doi.org/10.1016/j.neubiorev.2016.06.033

4. Conde, V., Palomar, F. J., Lama, M. J., Martínez, R., Carrillo, F., Pintado, E., & Mir, P. (2013). Abnormal GABA-mediated and cerebellar inhibition in women with the fragile X premutation. *Journal of Neurophysiology*, *109*(5), 1315–1322. https://doi.org/10.1152/jn.00730.2012

5. Copping, N. A., Adhikari, A., Petkova, S. P., & Silverman, J. L. (2019). Genetic backgrounds have unique seizure response profiles and behavioral outcomes following convulsant administration. Epilepsy & Behavior, 101, 106547. https://doi.org/10.1016/j.yebeh.2019.106547

6. Crawford, D. C., Acuña, J. M., & Sherman, S. L. (2001). FMR1 and the fragile X syndrome: Human genome epidemiology review. Genetics in Medicine, 3(5), 359–371. https://doi.org/10.1097/00125817-200109000-00006

7. Dahlhaus, R., & El-Husseini, A. (2010). Altered neuroligin expression is involved in social deficits in a mouse model of the fragile X syndrome. *Behavioural Brain Research*, *208*(1), 96–105. https://doi.org/10.1016/j.bbr.2009.11.019

8. Danbolt, N. C. (2001). Glutamate uptake. *Progress in Neurobiology*, *65*(1), 1–105. https://doi.org/10.1016/s0301-0082(00)00067-8

9. Deng, W., Aimone, J. B., & Gage, F. H. (2010). New neurons and new memories: How does adult hippocampal neurogenesis affect learning and memory? Nature Reviews Neuroscience, 11(5), 339–350. https://doi.org/10.1038/nrn2822

10. Deng, P.-Y., & Klyachko, V. A. (2021). Channelopathies in fragile X syndrome. Nature Reviews Neuroscience, 22(5), 275–289. https://doi.org/10.1038/s41583-021-00445-9

11. Deng, P.-Y., Kumar, A., Cavalli, V., & Klyachko, V. A. (2022). FMRP regulates GABAA receptor channel activity to control signal integration in hippocampal granule cells. *Cell Reports*, *39*(7), 110820. https://doi.org/10.1016/j.celrep.2022.110820

12. D'Hulst, Charlotte, De Geest, N., Reeve, S. P., Van Dam, D., De Deyn, P. P., Hassan, B. A., & Kooy, R. F. (2006). Decreased expression of the Gabaa receptor in Fragile X syndrome. *Brain Research, 1121*(1), 238–245. https://doi.org/10.1016/j.brainres.2006.08.115

13. D'Hulst, C, & Kooy, R. F. (2009). Fragile X syndrome: From molecular genetics to therapy. *Journal of Medical Genetics*, *46*(9), 577–584. https://doi.org/10.1136/jmg.2008.064667

14. Elmariah, S. B., Oh, E. J., Hughes, E. G., & Balice-Gordon, R. J. (2005). Astrocytes regulate inhibitory synapse formation via TRK-mediated modulation of postsynaptic GABAareceptors. The Journal of Neuroscience, 25(14), 3638–3650. https://doi.org/10.1523/jneurosci.3980-04.2005

15. Ethridge, L. E., White, S. P., Mosconi, M. W., Wang, J., Byerly, M. J., & Sweeney, J. A. (2016). Reduced habituation of auditory evoked potentials indicate cortical hyper-excitability in fragile X syndrome. *Translational Psychiatry*, *6*(4). https://doi.org/10.1038/tp.2016.48

16. Fernández-Blanco, Á., & Dierssen, M. (2020). Rethinking intellectual disability from neuro- to Astro-Pathology. *International Journal of Molecular Sciences*, *21*(23), 9039. https://doi.org/10.3390/ijms21239039

17. Grossman, A. W., Aldridge, G. M., Lee, K. J., Zeman, M. K., Jun, C. S., Azam, H. S., Arii, T., Imoto, K., Greenough, W. T., & Rhyu, I. J. (2010). Developmental characteristics of dendritic spines in the dentate gyrus of FMR1 knockout mice. *Brain Research*, *1355*, 221–227. https://doi.org/10.1016/j.brainres.2010.07.090

18. Hagerman, R. J., Ono, M. Y., & Hagerman, P. J. (2005). Recent advances in Fragile X: A model for autism and neurodegeneration. *Current Opinion in Psychiatry*, *18*(5), 490–496. https://doi.org/10.1097/01.yco.0000179485.39520.b0

19. Hathaway WR, Newton BW. Neuroanatomy, Prefrontal Cortex. [Updated 2023 May 29]. In: StatPearls [Internet]. Treasure Island (FL): StatPearls Publishing; 2024 Jan-. Available from: https://www.ncbi.nlm.nih.gov/books/NBK499919/

20. Higashimori, H., Morel, L., Huth, J., Lindemann, L., Dulla, C., Taylor, A., Freeman, M., & Yang, Y. (2013). Astroglial FMRP-dependent translational down-regulation of mglur5 underlies glutamate transporter GLT1 dysregulation in the fragile X Mouse. *Human Molecular Genetics*, *22*(10), 2041–2054. https://doi.org/10.1093/hmg/ddt055

21. Higashimori, H., Schin, C. S., Chiang, M. S., Morel, L., Shoneye, T. A., Nelson, D. L., & Yang, Y. (2016). Selective Deletion of Astroglial FMRP Dysregulates Glutamate Transporter GLT1 and Contributes to Fragile X Syndrome Phenotypes In Vivo. The Journal of neuroscience : the official journal of the Society for Neuroscience, 36(27), 7079–7094. https://doi.org/10.1523/JNEUROSCI.1069-16.2016

22. Hodges, J. L., Yu, X., Gilmore, A., Bennett, H., Tjia, M., Perna, J. F., Chen, C.-C., Li, X., Lu, J., & Zuo, Y. (2017). Astrocytic contributions to synaptic and learning abnormalities in a mouse model of fragile X syndrome. *Biological Psychiatry*, *82*(2), 139–149. https://doi.org/10.1016/j.biopsych.2016.08.036

23. Hösli, L., Binini, N., Ferrari, K. D., Thieren, L., Looser, Z. J., Zuend, M., Zanker, H. S., Berry, S., Holub, M., Möbius, W., Ruhwedel, T., Nave, K.-A., Giaume, C., Weber, B., & Saab, A. S. (2022). Decoupling astrocytes in adult mice impairs synaptic plasticity and spatial learning. *Cell Reports*, *38*(10), 110484. https://doi.org/10.1016/j.celrep.2022.110484

24. Huber, K. M., Gallagher, S. M., Warren, S. T., & Bear, M. F. (2002). Altered synaptic plasticity in a mouse model of fragile x mental retardation. *Proceedings of the National Academy of Sciences*, *99*(11), 7746–7750. https://doi.org/10.1073/pnas.122205699

25. Hutsler, J. J., & Zhang, H. (2010). Increased dendritic spine densities on cortical projection neurons in autism spectrum disorders. *Brain Research*, *1309*, 83–94. https://doi.org/10.1016/j.brainres.2009.09.120

26. Irwin, S. A. (2000). Dendritic spine structural anomalies in fragile-X mental retardation syndrome. *Cerebral Cortex*, *10*(10), 1038–1044. https://doi.org/10.1093/cercor/10.10.1038

27. Jacobs, S., & Doering, L. C. (2010). Astrocytes prevent abnormal neuronal development in the fragile X Mouse. *The Journal of Neuroscience*, *30*(12), 4508–4514. https://doi.org/10.1523/jneurosci.5027-09.2010

28. Jacobs, S., Nathwani, M., & Doering, L. C. (2010). Fragile X astrocytes induce developmental delays in dendrite maturation and synaptic protein expression. *BMC Neuroscience*, *11*(1). https://doi.org/10.1186/1471-2202-11-132

29. Jin, S., Higashimori, H., Schin, C., Tamashiro, A., Men, Y., Chiang, M. S., Jarvis, R., Cox, D., Feig, L., & Yang, Y. (2020). Astroglial fmrp modulates synaptic signaling and behavior phenotypes in fxs mouse model. *Glia*, *69*(3), 594–608. https://doi.org/10.1002/glia.23915

30. Kaidanovich-Beilin, O., Lipina, T., Vukobradovic, I., Roder, J., & Woodgett, J. R. (2011). Assessment of Social Interaction Behaviors. *Journal of Visualized Experiments*, (48). https://doi.org/10.3791/2473

31. Kau, A. S. M., Tierney, E., Bukelis, I., Stump, M. H., Kates, W. R., Trescher, W. H., & Kaufmann, W. E. (2004a). Social Behavior Profile in young males with fragile X syndrome: Characteristics and specificity. *American Journal of Medical Genetics Part A*, *126A*(1), 9–17. https://doi.org/10.1002/ajmg.a.20218

32. Kirchgessner, C. U., Warren, S. T., & Willard, H. F. (1995). X inactivation of the FMR1 fragile X mental retardation gene. Journal of medical genetics, 32(12), 925–929. https://doi.org/10.1136/jmg.32.12.925

33. Kraeuter, A.-K., Guest, P. C., & Sarnyai, Z. (2018). The elevated plus maze test for measuring anxiety-like behavior in rodents. *Methods in Molecular Biology*, 69–74. https://doi.org/10.1007/978-1-4939-8994-2_4

34. Ligsay, A., & Hagerman, R. J. (2016). Review of targeted treatments in fragile X syndrome. Intractable & Rare Diseases Research, 5(3), 158–167. https://doi.org/10.5582/irdr.2016.01045

35. Liu, X., Ying, J., Wang, X., Zheng, Q., Zhao, T., Yoon, S., Yu, W., Yang, D., Fang, Y., & Hua, F. (2021). Astrocytes in neural circuits: Key factors in synaptic regulation and potential targets for neurodevelopmental disorders. *Frontiers in Molecular Neuroscience*, *14*. https://doi.org/10.3389/fnmol.2021.729273

36. Liu, Z. H., Chuang, D. M., & Smith, C. B. (2011). Lithium ameliorates phenotypic deficits in a mouse model of fragile X syndrome. The international journal of neuropsychopharmacology, 14(5), 618–630. https://doi.org/10.1017/S1461145710000520

37. Maaswinkel, H., Baars, A.-M., Gispen, W.-H., & Spruijt, B. M. (1996). Roles of the basolateral amygdala and hippocampus in social recognition in rats. Physiology & Behavior, 60(1), 55–63. https://doi.org/10.1016/0031-9384(95)02233-3

38. Maddalena, A., Richards, C. S., McGinniss, M. J., Brothman, A., Desnick, R. J., Grier, R. E., Hirsch, B., Jacky, P., McDowell, G. A., Popovich, B., Watson, M., & Wolff, D. J. (2001). Technical standards and guidelines for Fragile X: The first of a series of disease-specific supplements to the standards and guidelines for Clinical Genetics Laboratories of the American College of Medical Genetics. Genetics in Medicine, 3(3), 200–205. https://doi.org/10.1097/00125817-200105000-00010

39. Martorell, L., Nascimento, M. T., Colome, R., Genovés, J., Naudó, M., & Nascimento, A. (2010). Four sisters compound heterozygotes for the pre- and full mutation in fragile X syndrome and a complete inactivation of X-functional chromosome: Implications for genetic counseling. *Journal of Human Genetics, 56*(1), 87–90. https://doi.org/10.1038/jhg.2010.140

40. Martorell, L., Nascimento, M. T., Colome, R., Genovés, J., Naudó, M., & Nascimento, A. (2010b). Four sisters compound heterozygotes for the pre- and full mutation in fragile X syndrome and a complete inactivation of X-functional chromosome: Implications for genetic counseling. *Journal of Human Genetics*, *56*(1), 87–90. https://doi.org/10.1038/jhg.2010.140

41. McNaughton, C. H., Moon, J., Strawderman, M. S., Maclean, K. N., Evans, J., & Strupp, B. J. (2008). Evidence for social anxiety and impaired social cognition in a mouse model of fragile X syndrome. Behavioral neuroscience, 122(2), 293–300. https://doi.org/10.1037/0735-7044.122.2.293

42. Mineur, Y.S., Sluyter, F., de Wit, S., Oostra, B.A. and Crusio, W.E. (2002), Behavioral and neuroanatomical characterization of the Fmr1 knockout mouse. Hippocampus, 12: 39-46. https://doi.org/10.1002/hipo.10005

43. Nielsen, D. M., Derber, W. J., McClellan, D. A., & Crnic, L. S. (2002). Alterations in the auditory startle response in FMR1 targeted mutant mouse models of fragile X syndrome. Brain Research, 927(1), 8–17. https://doi.org/10.1016/s0006-8993(01)03309-1

44. Nolin SL, Lewis FA III, Ye LL, Houck GE Jr, Glicksman AE, Limprasert P, Li SY, Zhong N, Ashley AE, Feingold E et al.: Familial transmission of the FMR1 CGG repeat. Am J Hum Genet 1996, 59:1252-1261.

45. Oliveira, J. F., Sardinha, V. M., Guerra-Gomes, S., Araque, A., & Sousa, N. (2015). Do stars govern our actions? Astrocyte involvement in rodent behavior. Trends in Neurosciences, 38(9), 535–549. https://doi.org/10.1016/j.tins.2015.07.006

46. Peier, A. M., McIlwain, K. L., Kenneson, A., Warren, S. T., Paylor, R., & Nelson, D. L. (2000). (over)correction of FMR1 deficiency with YAC transgenics:

Behavioral and physical features. *Human Molecular Genetics*, *9*(8), 1145–1159. https://doi.org/10.1093/hmg/9.8.1145

47. Pembrey, M. E., Barnicoat, A. J., Carmichael, B., Bobrow, M., & Turner, G. (2001). An assessment of screening strategies for Fragile X syndrome in the UK. *Health Technology Assessment*, *5*(7). https://doi.org/10.3310/hta5070

48. Penagarikano, O., Mulle, J. G., & Warren, S. T. (2007). The Pathophysiology of Fragile X Syndrome. *Annual Review of Genomics and Human Genetics*, *8*(1), 109–129. https://doi.org/10.1146/annurev.genom.8.080706.092249

49. Pfeiffer, B. E., & Huber, K. M. (2009). The State of Synapses in Fragile X Syndrome. The Neuroscientist : A Review Journal Bringing Neurobiology, Neurology and Psychiatry, 15(5), 549–567. https://doi.org/10.1177/1073858409333075

50. Protic, D. D., Aishworiya, R., Salcedo-Arellano, M. J., Tang, S. J., Milisavljevic, J., Mitrovic, F., Hagerman, R. J., & Budimirovic, D. B. (2022a). Fragile X syndrome: From Molecular Aspect to Clinical Treatment. International Journal of Molecular Sciences, 23(4), 1935. https://doi.org/10.3390/ijms23041935

51. Rais, M., Binder, D. K., Razak, K. A., & Ethell, I. M. (2018). Sensory processing phenotypes in Fragile X syndrome. ASN Neuro, 10, 175909141880109. https://doi.org/10.1177/1759091418801092

52. Reiss, A. L., & Hall, S. S. (2007). Fragile X syndrome: Assessment and treatment implications. *Child and Adolescent Psychiatric Clinics of North America*, *16*(3), 663–675. https://doi.org/10.1016/j.chc.2007.03.001

53. Salcedo-Arellano, M. J., Hagerman, R., & Martinez Cerdeno, V. (2020). Fragile X syndrome: Clinical presentation, pathology and treatment. Gaceta Medica de Mexico, 156. https://doi.org/10.24875/GMM.M19000322

54. Sandoval, G. M., Shim, S., Hong, D. S., Garrett, A. S., Quintin, E.-M., Marzelli, M. J., Patnaik, S., Lightbody, A. A., & Reiss, A. L. (2018). Neuroanatomical abnormalities in fragile X syndrome during the adolescent and young adult years. Journal of Psychiatric Research, 107, 138–144. https://doi.org/10.1016/j.jpsychires.2018.10.014

55. Schindelin, J., Arganda-Carreras, I., Frise, E., Kaynig, V., Longair, M., Pietzsch, T., … Cardona, A. (2012). Fiji: an open-source platform for biological-image analysis. Nature Methods, 9(7), 676–682. doi:10.1038/nmeth.2019

56. Schousboe, A., & Waagepetersen, H. S. (2005). Role of astrocytes in glutamate homeostasis: Implications for excitotoxicity. *Neurotoxicity Research*, *8*(3–4), 221–225. https://doi.org/10.1007/bf03033975

57. Seibenhener, M. L., & Wooten, M. C. (2015). Use of the open field maze to measure locomotor and anxiety-like behavior in mice. *Journal of Visualized Experiments*, (96). https://doi.org/10.3791/52434

58. Sherman S: Epidemiology. In Fragile X Syndrome: Diagnosis, Treatment and Research, edn 3. Edited by Hagerman RJ, Hagerman PJ: Baltimore, MD: The Johns Hopkins University Press; 2002:136-168.

59. Sieghart, W., Fuchs, K., Tretter, V., Ebert, V., Jechlinger, M., Höger, H., & Adamiker, D. (1999). Structure and subunit composition of Gabaa receptors. *Neurochemistry International*, *34*(5), 379–385. https://doi.org/10.1016/s0197-0186(99)00045-5

60. Stone, W. L., Basit, H., Shah, M., & Los, E. (2023). *National Library of Medicine*. https://www.ncbi.nlm.nih.gov/books/NBK459243/

61. Straub, D., Schmitt, L. M., Boggs, A. E., Horn, P. S., Dominick, K. C., Gross, C., & Erickson, C. A. (2023). A sensitive and reproducible QRT-PCR assay detects physiological relevant trace levels of FMR1 mrna in individuals with fragile X syndrome. *Scientific Reports*, *13*(1). https://doi.org/10.1038/s41598-023-29786-4

62. Sutcliffe, J. S., Nelson, D. L., Zhang, F., Pieretti, M., Caskey, C. T., Saxe, D., & Warren, S. T. (1992). DNA methylation represses fmr-1 transcription in Fragile X syndrome. Human Molecular Genetics, 1(6), 397–400. https://doi.org/10.1093/hmg/1.6.397

63. Tanaka, K., Watase, K., Manabe, T., Yamada, K., Watanabe, M., Takahashi, K., Iwama, H., Nishikawa, T., Ichihara, N., Kikuchi, T., Okuyama, S., Kawashima, N., Hori, S., Takimoto, M., & Wada, K. (1997). Epilepsy and exacerbation of brain injury in mice lacking the glutamate transporter GLT-1. *Science*, *276*(5319), 1699–1702. https://doi.org/10.1126/science.276.5319.1699

64. THE DUTCH-BELGIAN FRAGILE X CONSORTHIUM. (1994). FMR1 knockout mice: A model to study fragile X mental retardation. *Cell*, *78*(1). https://doi.org/10.1016/0092-8674(94)90569-x

65. Turner, G., Webb, T., Wake, S. and Robinson, H. (1996), Prevalence of fragile X syndrome. Am. J. Med. Genet., 64: 196-197. https://doi.org/10.1002/(SICI)1096-8628(19960712)64:1<196::AID-AJMG35>3.0.CO;2-G

66. Verkhratsky, A., Zorec, R., & Parpura, V. (2017). Stratification of astrocytes in healthy and diseased brain. *Brain Pathology*, *27*(5), 629–644. https://doi.org/10.1111/bpa.12537

67. von Bartheld, C. S., Bahney, J., & Herculano-Houzel, S. (2016). The search for true numbers of neurons and glial cells in the human brain: A review of 150 years of cell counting. *Journal of Comparative Neurology*, *524*(18), 3865–3895. https://doi.org/10.1002/cne.24040

68. Wang, J., Ethridge, L. E., Mosconi, M. W., White, S. P., Binder, D. K., Pedapati, E. V., Erickson, C. A., Byerly, M. J., & Sweeney, J. A. (2017). A resting EEG study of neocortical hyperexcitability and altered functional connectivity in fragile X syndrome. *Journal of Neurodevelopmental Disorders*, *9*(1). https://doi.org/10.1186/s11689-017-9191-z

69. Yan, Q. J., Asafo-Adjei, P. K., Arnold, H. M., Brown, R. E., & Bauchwitz, R. P. (2004). A phenotypic and molecular characterization of the *fmr1-tm1cgr* fragile X mouse. *Genes, Brain and Behavior*, *3*(6), 337–359. https://doi.org/10.1111/j.1601-183x.2004.00087.x

70. Yong, A. J., Tan, H. L., Zhu, Q., Bygrave, A. M., Johnson, R. C., & Huganir, R. L. (2020). Tyrosine phosphorylation of the AMPA receptor subunit GLUA2 gates homeostatic synaptic plasticity. *Proceedings of the National Academy of Sciences*, *117*(9), 4948–4958. https://doi.org/10.1073/pnas.1918436117

71. Yuskaitis, C. J., Mines, M. A., King, M. K., Sweatt, J. D., Miller, C. A., & Jope, R. S. (2010a). Lithium ameliorates altered glycogen synthase kinase-3 and behavior in a mouse model of fragile X syndrome. *Biochemical Pharmacology*, *79*(4), 632–646. https://doi.org/10.1016/j.bcp.2009.09.023

72. Zhang, Z., Ma, Z., Zou, W., Guo, H., Liu, M., Ma, Y., & Zhang, L. (2019). The appropriate marker for astrocytes: Comparing the distribution and expression of three astrocytic markers in different mouse cerebral regions. BioMed Research International, 2019, 1–15. https://doi.org/10.1155/2019/9605265

APPENDIX A

Supplemental Information

Supplementary Tables

Table S1: Summary table showing Velocity in the Whole Arena during the Open Field Test (OFT). Velocity was calculated in mm/second for WT/cKO males and HET/cKO Females, and interactions between genotype and sex were investigated. Statistical analysis of the differences between sex and the astrocyte-specific cKO and its WT/HET counterparts was performed using a Two-Way ANOVA followed by a Tukey multiple-comparison post-test: *P < 0.05, **P < 0.01.

0-5 Minutes

Group	df	MS	F (DFn, DFd)	p	p value Summary
Interaction	1	6.661	F (1, 85) = 0.2716	0.6036	ns
Genotype	1	190.2	F (1, 85) = 7.753	0.0066	**
Sex	1	4.884	F (1, 85) = 0.1991	0.6566	ns

5-10 Minutes

Group	df	MS	F (DFn, DFd)	p	p value Summary
Interaction	1	0.0392	F (1, 83) = 0.002538	P=0.9599	ns
Genotype	1	143.5	F (1, 83) = 9.287	P=0.0031	**
Sex	1	0.03502	F (1, 83) = 0.002267	P=0.9621	ns

Full 10 Minutes

Group	df	MS	F (DFn, DFd)	p	p value Summary
Interaction	1	2.033	F (1, 83) = 0.1178	P=0.7323	ns
Genotype	1	164.2	F (1, 83) = 9.510	P=0.0028	**
Sex	1	1.527	F (1, 83) = 0.08845	P=0.7669	ns

Table S2: Summary table showing Distance in the Whole Arena during the Open Field Test (OFT). Distance traveled was determined in millimeters (mm) for WT/cKO males and HET/cKO Females, and interactions between genotype and sex were investigated. Statistical analysis of the differences between sex and the astrocyte-specific cKO and its WT/HET counterparts was performed using a Two-Way ANOVA followed by a Tukey multiple-comparison post-test: *P < 0.05, **P < 0.01.

0-5 Minutes

Group	df	MS	F (DFn, DFd)	p	p value Summary
Interaction	1	637816	F (1, 85) = 0.2947	P=0.5886	ns
Genotype	1	16436112	F (1, 85) = 7.595	P=0.0072	**
Sex	1	381381	F (1, 85) = 0.1762	P=0.6757	ns

5-10 Minutes

Group	df	MS	F (DFn, DFd)	p	p value Summary
Interaction	1	3281	F (1, 83) = 0.002405	P=0.9610	ns
Genotype	1	12690116	F (1, 83) = 9.304	P=0.0031	**
Sex	1	4795	F (1, 83) = 0.003516	P=0.9529	ns

Full 10 Minutes

Group	df	MS	F (DFn, DFd)	p	p value Summary
Interaction	1	770675	F (1, 83) = 0.1265	P=0.7230	ns
Genotype	1	57371516	F (1, 83) = 9.415	P=0.0029	**
Sex	1	503429	F (1, 83) = 0.08262	P=0.7745	ns

Table S3: Summary table showing Velocity in Thigmotaxis during the Open Field Test (OFT). Velocity was calculated in mm/second for WT/cKO males and HET/cKO Females, and interactions between genotype and sex were investigated. Statistical analysis of the differences between sex and the astrocyte-specific cKO and its WT/HET counterparts was performed using a Two-Way ANOVA followed by a Tukey multiple-comparison post-test: *P < 0.05, **P < 0.01.

0-5 Minutes

Group	df	MS	F (DFn, DFd)	p	p value Summary
Interaction	1	12.01	F (1, 85) = 0.4588	P=0.5000	ns
Genotype	1	269.4	F (1, 85) = 10.29	P=0.0019	**
Sex	1	1.381	F (1, 85) = 0.05274	P=0.8189	ns

5-10 Minutes

Group	df	MS	F (DFn, DFd)	p	p value Summary
Interaction	1	0.3226	F (1, 83) = 0.01747	P=0.8952	ns
Genotype	1	175.2	F (1, 83) = 9.486	P=0.0028	**
Sex	1	2.164	F (1, 83) = 0.1172	P=0.7330	ns

Full 10 Minutes

Group	df	MS	F (DFn, DFd)	p	p value Summary
Interaction	1	3.855	F (1, 83) = 0.1982	P=0.6573	ns
Genotype	1	220.2	F (1, 83) = 11.32	P=0.0012	**
Sex	1	1.868	F (1, 83) = 0.09607	P=0.7574	ns

Table S4: Summary table showing Distance in Thigmotaxis during the Open Field Test (OFT). Distance traveled was determined in millimeters (mm) for WT/cKO males and HET/cKO Females, and interactions between genotype and sex were investigated. Statistical analysis of the differences between sex and the astrocyte-specific cKO and its WT/HET counterparts was performed using a Two-Way ANOVA followed by a Tukey multiple-comparison post-test: *P < 0.05, **P < 0.01.

0-5 Minutes

Group	df	MS	F (DFn, DFd)	p	p value Summary
Interaction	1	1150326	F (1, 85) = 0.4884	P=0.4866	ns
Genotype	1	25234607	F (1, 85) = 10.71	P=0.0015	**
Sex	1	117885	F (1, 85) = 0.05005	P=0.8235	ns

5-10 Minutes

Group	df	MS	F (DFn, DFd)	p	p value Summary
Interaction	1	29037	F (1, 83) = 0.01747	P=0.8952	ns
Genotype	1	15769464	F (1, 83) = 9.486	P=0.0028	**
Sex	1	194756	F (1, 83) = 0.1172	P=0.7330	ns

Full 10 Minutes

Group	df	MS	F (DFn, DFd)	p	p value Summary
Interaction	1	1387702	F (1, 83) = 0.1982	P=0.6573	ns
Genotype	1	79260895	F (1, 83) = 11.32	P=0.0012	**
Sex	1	672592	F (1, 83) = 0.09607	P=0.7574	ns

Table S5: Summary table showing % of Time Spent in the Open Field during the Open Field Test (OFT). The % of Time Spent in the Open Field was determined for the WT/cKO males and HET/cKO Females, and interactions between genotype and sex were investigated. Statistical analysis of the differences between sex and the astrocyte-specific cKO and its WT/HET counterparts was performed using a Two-Way ANOVA followed by a Tukey multiple-comparison post-test: *P < 0.05, **P < 0.01.

0-5 Minutes

Group	df	MS	F (DFn, DFd)	p	p value Summary
Interaction	1	167.9	F (1, 85) = 1.664	P=0.2006	ns
Genotype	1	285.9	F (1, 85) = 2.833	P=0.0960	ns
Sex	1	36.76	F (1, 85) = 0.3642	P=0.5478	ns

5-10 Minutes

Group	df	MS	F (DFn, DFd)	p	p value Summary
Interaction	1	114.5	F (1, 83) = 0.7290	P=0.3957	ns
Genotype	1	668.7	F (1, 83) = 4.257	P=0.0422	*
Sex	1	22.22	F (1, 83) = 0.1415	P=0.7078	ns

Full 10 Minutes

Group	df	MS	F (DFn, DFd)	p	p value Summary
Interaction	1	2.365	F (1, 83) = 0.02295	P=0.8799	ns
Genotype	1	444.6	F (1, 83) = 4.315	P=0.0409	*
Sex	1	0.05959	F (1, 83) = 0.0005784	P=0.9809	ns

Table S6: Summary table showing % of Time Spent in Thigmotaxis during the Open Field Test (OFT). The % of Time Spent in Thigmotaxis was determined for the WT/cKO males and HET/cKO Females, and interactions between genotype and sex were investigated. Statistical analysis of the differences between sex and the astrocyte-specific cKO and its WT/HET counterparts was performed using a Two-Way ANOVA followed by a Tukey multiple-comparison post-test: *P < 0.05, **P < 0.01.

0-5 Minutes

Group	df	MS	F (DFn, DFd)	p	p value Summary
Interaction	1	228.9	F (1, 85) = 2.119	P=0.1492	ns
Genotype	1	284.2	F (1, 85) = 2.631	P=0.1085	ns
Sex	1	47.91	F (1, 85) = 0.4435	P=0.5072	ns

5-10 Minutes

Group	df	MS	F (DFn, DFd)	p	p value Summary
Interaction	1	59.79	F (1, 83) = 0.3638	P=0.5481	ns
Genotype	1	609.9	F (1, 83) = 3.711	P=0.0575	ns
Sex	1	3.895	F (1, 83) = 0.02370	P=0.8780	ns

Full 10 Minutes

Group	df	MS	F (DFn, DFd)	p	p value Summary
Interaction	1	10.3	F (1, 83) = 0.09402	P=0.7599	ns
Genotype	1	450.4	F (1, 83) = 4.113	P=0.0458	*
Sex	1	8.512	F (1, 83) = 0.07774	P=0.7811	ns

Table S7: Summary table showing Velocity in Whole Arena during the Elevated Plus Maze Test (EPM). The Velocity in mm/s was determined for the WT/cKO males and HET/cKO Females, and interactions between genotype and sex were investigated. Statistical analysis of the differences between sex and the astrocyte-specific cKO and its WT/HET counterparts was performed using a Two-Way ANOVA followed by a Tukey multiple-comparison post-test: *P < 0.05, **P < 0.01.

0-5 Minutes

Group	df	MS	F (DFn, DFd)	p	p value Summary
Interaction	1	7.587	F (1, 78) = 0.6467	P=0.4237	ns
Genotype	1	2.669	F (1, 78) = 0.2275	P=0.6347	ns
Sex	1	0.06901	F (1, 78) = 0.005882	P=0.9391	ns

5-10 Minutes

Group	df	MS	F (DFn, DFd)	p	p value Summary
Interaction	1	0.1345	F (1, 75) = 0.02398	P=0.8774	ns
Genotype	1	12.9	F (1, 75) = 2.300	P=0.1336	ns
Sex	1	4.449	F (1, 75) = 0.7929	P=0.3761	ns

Full 10 Minutes

Group	df	MS	F (DFn, DFd)	p	p value Summary
Interaction	1	2.065	F (1, 75) = 0.3778	P=0.5406	ns
Genotype	1	7.974	F (1, 75) = 1.459	P=0.2308	ns
Sex	1	0.4512	F (1, 75) = 0.08257	P=0.7746	ns

Table S8: Summary table showing the % Time Spent in Open Arms during the Elevated Plus Maze Test (EPM). The % Time was determined for the WT/cKO males and HET/cKO Females, and interactions between genotype and sex were investigated. Statistical analysis of the differences between sex and the astrocyte-specific cKO and its WT/HET counterparts was performed using a Two-Way ANOVA followed by a Tukey multiple-comparison post-test: *P < 0.05, **P < 0.01.

0-5 Minutes

Group	df	MS	F (DFn, DFd)	p	p value Summary
Interaction	1	110.5	F (1, 77) = 1.820	P=0.1812	ns
Genotype	1	32.8	F (1, 77) = 0.5406	P=0.4644	ns
Sex	1	78.13	F (1, 77) = 1.288	P=0.2600	ns

5-10 Minutes

Group	df	MS	F (DFn, DFd)	p	p value Summary
Interaction	1	8.548	F (1, 72) = 0.1231	P=0.7267	ns
Genotype	1	2.013	F (1, 72) = 0.02900	P=0.8652	ns
Sex	1	135.3	F (1, 72) = 1.949	P=0.1669	ns

Full 10 Minutes

Group	df	MS	F (DFn, DFd)	p	p value Summary
Interaction	1	42.68	F (1, 73) = 1.109	P=0.2957	ns
Genotype	1	7.01	F (1, 73) = 0.1822	P=0.6707	ns
Sex	1	70.44	F (1, 73) = 1.831	P=0.1802	ns

Table S9: Summary table showing the % Time Spent in Closed Arms during the Elevated Plus Maze Test (EPM). The % Time was determined for the WT/cKO males and HET/cKO Females, and interactions between genotype and sex were investigated. Statistical analysis of the differences between sex and the astrocyte-specific cKO and its WT/HET counterparts was performed using a Two-Way ANOVA followed by a Tukey multiple-comparison post-test: *P < 0.05, **P < 0.01.

0-5 Minutes

Group	df	MS	F (DFn, DFd)	p	p value Summary
Interaction	1	119.6	F (1, 77) = 1.942	P=0.1674	ns
Genotype	1	27.87	F (1, 77) = 0.4525	P=0.5032	ns
Sex	1	69.98	F (1, 77) = 1.136	P=0.2898	ns

5-10 Minutes

Group	df	MS	F (DFn, DFd)	p	p value Summary
Interaction	1	8.653	F (1, 72) = 0.1246	P=0.7251	ns
Genotype	1	1.963	F (1, 72) = 0.02827	P=0.8669	ns
Sex	1	135.7	F (1, 72) = 1.955	P=0.1663	ns

Full 10 Minutes

Group	df	MS	F (DFn, DFd)	p	p value Summary
Interaction	1	45.52	F (1, 73) = 1.164	P=0.2841	ns
Genotype	1	5.8	F (1, 73) = 0.1484	P=0.7012	ns
Sex	1	66.77	F (1, 73) = 1.708	P=0.1953	ns

Table S10: Summary table showing Sociability Index the Social Novelty Test (SNT). The Sociability Index was determined for the WT/cKO males and HET/cKO Females, and interactions between genotype and sex were investigated. Statistical analysis of the differences between sex and the astrocyte-specific cKO and its WT/HET counterparts was performed using a Two-Way ANOVA followed by a Tukey multiple-comparison post-test: *P < 0.05, **P < 0.01.

0-5 Minutes

Group	df	MS	F (DFn, DFd)	p	p value Summary
Interaction	1	0.01281	F (1, 79) = 0.3107	P=0.5789	ns
Genotype	1	0.01672	F (1, 79) = 0.4056	P=0.5261	ns
Sex	1	0.01255	F (1, 79) = 0.3043	P=0.5827	ns

5-10 Minutes

Group	df	MS	F (DFn, DFd)	p	p value Summary
Interaction	1	0.01836	F (1, 78) = 0.7575	P=0.3868	ns
Genotype	1	0.07974	F (1, 78) = 3.290	P=0.0735	ns
Sex	1	0.07234	F (1, 78) = 2.985	P=0.0880	ns

Full 10 Minutes

Group	df	MS	F (DFn, DFd)	p	p value Summary
Interaction	1	0.000704	F (1, 76) = 0.04420	P=0.8340	ns
Genotype	1	0.003719	F (1, 76) = 0.2335	P=0.6303	ns
Sex	1	0.03031	F (1, 76) = 1.903	P=0.1718	ns

Table S11: Summary table showing Social Novelty Preference in the Social Novelty Test (SNT). The Social Novelty Preference Index was determined for the WT/cKO males and HET/cKO Females, and interactions between genotype and sex were investigated. Statistical analysis of the differences between sex and the astrocyte-specific cKO and its WT/HET counterparts was performed using a Two-Way ANOVA followed by a Tukey multiple-comparison post-test: *P < 0.05, **P < 0.01.

0-5 Minutes

Group	df	MS	F (DFn, DFd)	p	p value Summary
Interaction	1	0.002417	F (1, 81) = 0.09463	P=0.7592	ns
Genotype	1	0.01369	F (1, 81) = 0.5360	P=0.4662	ns
Sex	1	0.03481	F (1, 81) = 1.363	P=0.2465	ns

5-10 Minutes

Group	df	MS	F (DFn, DFd)	p	p value Summary
Interaction	1	0.02763	F (1, 78) = 0.8955	P=0.3469	ns
Genotype	1	0.02109	F (1, 78) = 0.6835	P=0.4109	ns
Sex	1	0.01578	F (1, 78) = 0.5113	P=0.4767	ns

Full 10 Minutes

Group	df	MS	F (DFn, DFd)	p	p value Summary
Interaction	1	0.001029	F (1, 77) = 0.05399	P=0.8169	ns
Genotype	1	0.000129	F (1, 77) = 0.006772	P=0.9346	ns
Sex	1	0.000547	F (1, 77) = 0.02869	P=0.8660	ns

Table S12: Summary table showing % Time Spent with Stranger 1 in the First 5 Minutes in the Social Novelty Test (SNT). This time was determined for the WT/cKO males and HET/cKO Females, and interactions between genotype and sex were investigated. Statistical analysis of the differences between sex and the astrocyte-specific cKO and its WT/HET counterparts was performed using a Two-Way ANOVA followed by a Tukey multiple-comparison post-test: *P < 0.05, **P < 0.01.

Group	df	MS	F (DFn, DFd)	p	p value Summary
Interaction	1	300.3	F (1, 78) = 1.255	P=0.2661	ns
Genotype	1	312	F (1, 78) = 1.303	P=0.2571	ns
Sex	1	43.95	F (1, 78) = 0.1836	P=0.6695	ns

Table S13: Summary table showing % Time Spent with Stranger 2 in the First 5 Minutes in the Social Novelty Test (SNT). This time was determined for the WT/cKO males and HET/cKO Females, and interactions between genotype and sex were investigated. Statistical analysis of the differences between sex and the astrocyte-specific cKO and its WT/HET counterparts was performed using a Two-Way ANOVA followed by a Tukey multiple-comparison post-test: *P < 0.05, **P < 0.01.

Group	df	MS	F (DFn, DFd)	p	p value Summary
Interaction	1	225.4	F (1, 78) = 1.537	P=0.2187	ns
Genotype	1	316.4	F (1, 78) = 2.158	P=0.1458	ns
Sex	1	704.3	F (1, 78) = 4.805	P=0.0314	*

Supplementary Graphs

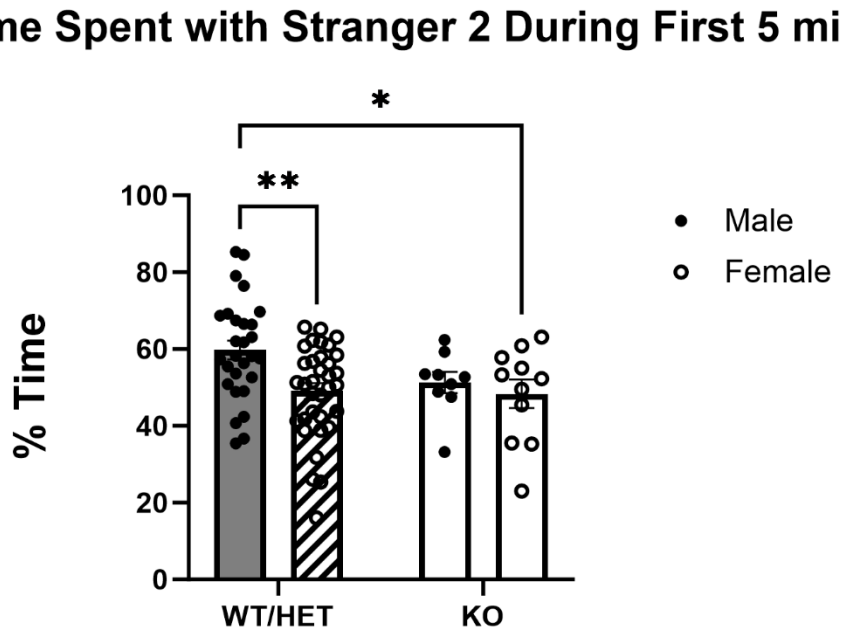

Figure S1: Graphs describe the Percent Time Spent with Stranger 2 During the First 5 Minutes of the Social Novelty Test (SNT). % Time Spent with Stranger 2 During First 5 Minutes. Observed differences in % time spent with Stranger 2 between the WT and HET and the WT and the female High Cre cKO. There are no significant differences between the HET and both the male and female High Cre cKO groups. The WT group spends a larger percentage of time with Stranger 1 in the first 5 minutes of the test compared to the HET, male High Cre cKO, and the female High Cre cKO. (WT N = 32, HET N= 36, Male cKO N = 10, Female cKO N = 11; *P < 0.05; **P < 0.01; Two-Way ANOVA followed by a Tukey multiple-comparison post-test).